Polyethylene glycol (PEG)-associated immunological effects triggered by clinically relevant lipid nanoparticles

Haiyang Wang[1,2†], Yisha Wang[1,2†], Changzheng Yuan[3†], Xiao Xu[4], Wenbin Zhou[1,2], Yuhui Huang[3], Huan Lu[1,2], Yue Zheng[1,2], Gan Luo[1,2], Jia Shang[1,2], Meihua Sui[1,2*]

[1]School of Basic Medical Sciences and Women's Hospital, Zhejiang University School of Medicine, Hangzhou, China
[2]Cancer Center, Zhejiang University, Hangzhou, China.
[3]School of Public Health, Zhejiang University School of Medicine, Hangzhou, China.
[4]Key Laboratory of Integrated Oncology and Intelligent Medicine of Zhejiang Province, Department of Hepatobiliary and Pancreatic Surgery, Affiliated Hangzhou First People's Hospital, Zhejiang University School of Medicine, Hangzhou, 310006, China

†Equal contribution

***Corresponding author**
Meihua Sui, M.D., Ph.D. **E-mail:** suim@zju.edu.cn

Abstract

Polyethylene glycol (PEG)-conjugated lipid has significantly contributed to the success of three approved lipid nanoparticles (LNP)-delivered therapeutics, particularly two COVID-19 mRNA vaccines. It is known that some PEG derivatives could elicit anti-PEG antibodies and subsequently form "antigen-antibody" complexes with newly injected PEGylated agents, leading to pharmacokinetic changes, reduced therapeutic efficacy and even hypersensitivity reactions. With the large-scale vaccination of mRNA vaccines, it has become an imminent task to elucidate the possible PEG-associated immunological effects induced by clinically relevant LNP. Up to date there are only four related studies, all of which are clinical observations emphasizing on the changes of PEG-specific antibodies upon injection of mRNA vaccines. Unfortunately, contradictory and inconclusive data were obtained due to significant person-to-person and study-to-study variabilities. To clarify the PEG-associated immunological effects of clinically relevant LNP in a model system with least "noise", we initiated an animal study using the PEGylated LNP of BNT162b2 (with the largest number of recipients) as a representative LNP and simulated the clinical practice. Through designing a series of time points and three doses correlated with the PEG amount contained in three approved LNP-based drugs, we demonstrated that generation and changes of anti-PEG IgM and IgG were time- and dose-dependent. Unexpectedly, our data revealed that unlike other PEG derivatives belonging to thymus-independent antigens (TI-Ag), PEGylated LNP not only induced isotype switch and production of anti-PEG IgG, but caused immune memory, leading to rapid enhancement and longer lasting time of both anti-PEG IgM and IgG upon repeated injection. Importantly, pharmacokinetic studies discovered that initial injection of PEGylated LNP accelerated the blood clearance of subsequently injected LNP. These findings will refresh our understandings on PEGylated LNP and possible other PEG derivatives, and may lead to optimization of both premarket guidelines and clinical protocols of PEGylated LNP-delivered therapeutics.

Introduction

Development of nucleic acid therapeutics has been restricted by the intrinsic defects of nucleic acids such as poor stability, immunogenicity and low penetration capability through cell membranes. Therefore, delivery platform possessing high stability, good targeting affinity and strong cellular internalization are urgently needed for therapeutic nucleic acids (*1*). Among various delivery systems for nucleic acids, lipid nanoparticles (LNP), which have four components including ionizable cationic lipid, cholesterol, 1,2-distearoyl-sn-glycero-3-phosphocholine (DSPC) and polyethylene glycol (PEG)-conjugated lipid (*2*), are of greatest attention due to unique advantages such as simple formulation, good biocompatibility, large payload and low toxic side effects (*3*). So far, there are three FDA-approved nucleic acid drugs using LNP as delivery vectors, namely Onpattro® (Patisiran, approved on August 10, 2018, an siRNA drug), the first COVID-19 mRNA vaccine Comirnaty® (BNT162b2, emergency use authorization approved on December 2, 2020) and the second COVID-19 mRNA vaccine Spikevax® (mRNA-1273, emergency use authorization approved on December 18, 2020) (*4*).

It has been demonstrated that modification of therapeutics with PEG, so called “PEGylation”, has multiple advantages such as increasing drug solubility and stability, reducing unfavorable immunogenicity and extending drug half-life (*5*). Indeed, as the first approved vaccine using PEG as an excipient, its PEG-conjugated lipid (ALC-0159) plays critical roles in improving the stability and prolonging blood circulation of LNP, which has significantly contributed to the overwhelming success of BNT162b2 in clinical trials (*6*). There used to be a general perception that PEG and its derivatives were nonimmunogenic. However, since anti-PEG IgM was first detected in rabbits immunized with PEGylated ovalbumin in 1983 (*7*), an expanding body of evidence has revealed that some PEG derivatives could elicit PEG-specific antibodies (*8-10*). Subsequently, anti-PEG antibodies may form "antigen-antibody" complexes with newly injected PEGylated agents. As a result, the immune complexes may be cleared by macrophage Fc receptor-mediated and complement receptor-mediated phagocytosis, leading to changes in the pharmacokinetics of newly injected PEGylated therapeutics and reduction of the drug efficacy (*8-11*). For instance, Dr. Roffler first demonstrated that anti-PEG IgM quickly cleared PEG-modified proteins from the blood in mice in 1999 (*12*). Later, Ishida T *et al.* proved that anti-PEG IgM elicited by an initial exposure to PEGylated liposomes triggered the accelerated blood clearance (ABC phenomenon) of subsequently administrated liposomes in rats *via* activation of the complement system (*13*). There are even clinical investigations demonstrating accelerated clearance of drugs triggered by anti-PEG antibodies and reduction of therapeutic efficacy (*14*, *15*).

With the large-scale vaccination of mRNA vaccine and the development of therapeutics using LNP as carriers, it has become an imminent task to elucidate the potential PEG-associated immunological effects induced by clinically relevant LNP. However, up to date there are only four related literatures, all of which are recent clinical observations including three reports based on mRNA vaccines: Alnylam Pharmaceuticals *Inc.* reported that anti-PEG IgM and IgG were induced in 3.4% of subjects (5 out of 145 patients) who received Patisiran in 2019 (*16*); Kent *et al.* reported

on June 27, 2022 that COVID-19 mRNA vaccines boosted the serum anti-PEG antibody levels in Australian recipients, with anti-PEG IgM boosted a mean of 2.64 folds and anti-PEG IgG boosted a mean of 1.78 folds following BNT162b2 vaccination (n=55), as well as anti-PEG IgM boosted a mean of 68.5 folds and anti-PEG IgG boosted a mean of 13.1 folds following mRNA-1273 vaccination (n=20) (*17*); Calzolai *et al.* from Joint Research Centre in Italy reported a significant increase in anti-PEG IgM level after the first injection of BNT162b2 and the third injection of BNT162b2 or mRNA-1273, while no boosting effect was observed on anti-PEG IgG after injection with either vaccine on August 9, 2022 (*18*); Krammer *et al* reported different response on induction of PEG-specific antibodies with a very small size of recipients in USA received either BNT162b2 or mRNA-1273 vaccination (n=10) on September 14, 2022 (*19*). It is noteworthy that as stated by the authors, pre-existing antibodies, small population sizes and inevitable interference due to exposure to PEG-containing substances other than vaccines after immunization may compromise the accuracy of clinical data, which may be responsible for the inconsistent results (*17, 19*). Moreover, the amount of mPEG2000 contained in each single injection varies significantly among the three FDA-approved LNP-delivered therapeutics (*20-22*). For instance, mPEG2000 contained in each injection of ONPATTRO is as high as 262 times of that in BNT162b2 (*20*), which has raised our concern on the potential impact of exposure amount over PEG-associated immunological effect induced by LNP. Another important aspect is that as the first vaccine using PEG as an excipient and LNP as a carrier, the *in vivo* pharmacokinetics of COVID-19 mRNA vaccine might differ from all other vaccines previously approved for clinical use, considering that the *in vivo* process of mRNA vaccine is mainly determined by its LNP vector (*21*). Unfortunately, until now there is still a lack of pharmacokinetic data of both BNT162b2 and mRNA-1273.

Motivated by these questions, we herein successfully synthesized the PEGylated LNP of BNT162b2, the most widely used LNP-delivered therapeutic, as a model LNP. DiR-labeled LNP (DiR@LNP) and DiR-labeled LNP encapsulating mRNA encoding the firefly luciferase (DiR-LU@LNP) were also prepared for visualization and *in vivo* quantitative studies. A Wistar rat model was selected, in order to take the advantage of well controlled animal studies to eliminate undesired exposure to PEG and its derivatives other than PEGylated LNP. Through simulating the clinical application of BNT162b2, *e.g.* two intramuscular injections with an interval of 21 days, we carefully characterized the model LNP in inducing PEG-associated immunological effects, *e.g.* dynamic changes in the subtypes and levels of anti-PEG antibodies. Importantly, three clinically relevant doses covering the whole range of PEG contained in a single injection of three FDA-approved LNP-delivered therapeutics, were delicately designed and studied, in order to assess the impact of PEG exposure amount on induction of anti-PEG antibodies. Moreover, potential pharmacokinetic changes caused by anti-PEG antibodies following repeated injection of PEGylated LNP were explored for the first time.

Results

Successful synthesis and physiochemical characterization of PEGylated LNP, DiR-LNP and

DiR-LU@LNP

As shown in Fig. 1A and Fig. 1B, as well as described in "Methods", LNP, DiR-LNP and DiR-LU@LNP were prepared by mixing of the ethanol phase (ALC-0315, DSPC, cholesterol and ALC-0159 in ethanol, with or without DiR) and the aqueous phase (citrate buffer with or without firefly luciferase mRNA) through a microfluidic mixing device. The obtained LNP formulations were first examined with Cryo-TEM, in which both LNP and DiR-LNP were hollow spheres, while DiR-LU@LNP had a typical electron-dense core structure containing mRNA (Fig. 1C). Next, LNP formulations were characterized with their Z-average (in neutral PBS), PDI (in neutral PBS) and surface Zeta potential (in ultrapure water) using DLS. As shown in Fig. 2A-2B and table S1, the Z-average/PDI/Zeta potential of LNP, DiR-LNP and DiR-LU@LNP were 110.400 ± 3.466 nm/0.203 ± 0.012/16.733 ± 0.451 mV, 113.067 ± 2.139 nm/0.183 ± 0.013/7.257 ± 0.168 mV and 101.367 ± 2.593 nm/0.197 ± 0.015/-5.943 ± 0.129 mV, respectively. These data demonstrate that all three types of LNP formulations have favorable particle diameter (around 100-110 nm), highly monodisperse particle-size distribution (PDI < 0.3), and weak surface charge (-5.943 mV~+ 16.733 mV) (*23, 24*).

As depicted in Fig. 2C and fig. S1, the Z-average/PDI of LNP formulations at four time points were as follows: LNP, 140.533 ± 2.768 nm/0.264 ± 0.012, 138.600 ± 0.100 nm/0.274 ± 0.005, 138.200 ± 0.954 nm/0.287 ± 0.013 and 141.867 ± 2.631 nm/0.287 ± 0.016 (Fig. 2C and fig. S1); DiR-LNP, 104.300 ± 0.458 nm/0.285 ± 0.014, 105.733 ± 0.503 nm/0.282 ± 0.010, 107.267 ± 1.940 nm/0.291 ± 0.013 and 117.200 ± 1.277 nm/0.392 ± 0.020 (Fig. 2D and fig. S2); DiR-LU@LNP, 135.067 ± 1.550 nm/0.240 ± 0.003, 133.867 ± 0.058 nm/0.251 ± 0.001, 132.667 ± 2.023 nm/0.246 ± 0.006 and 134.133 ± 1.222 nm/0.252 ± 0.006 (Fig. 2E and fig. S3). These data suggest that LNP, DiR-LNP and DiR-LU@LNP nanoparticles have relatively stable particle sizes and stay monodisperse *in vivo*.

Moreover, as the phospholipid component in LNP is commonly used for determining the amount of whole nanoparticles (*25, 26*), the standard curves of phospholipid (DSPC) in LNP, DiR-LNP and DiR-LU@LNP were respectively drawn and the following equations were obtained, in which y represents absorbance measured at 470 nm and x represents phospholipid concentration: y = 0.0077x+0.0098 (R^2 = 0.9914; Fig. 2F); y = 0.0076x+0.0244 (R^2 = 0.9909; Fig. 2G); y = 0.0071x+0.0284 (R^2 = 0.9841; Fig. 2H). These equations were used for subsequent calculation of three clinically relevant doses of LNP including low dose (L-LNP, 0.009 mg phospholipids/kg), middle dose (M-LNP, 0.342 mg phospholipids/kg) and high dose (H-LNP, 2.358 mg phospholipids/kg) (see "Methods").

Time- and dose-dependent induction of anti-PEG IgM antibody by PEGylated LNP

As shown in the schematic illustration (Fig. 3A), Wistar rats were respectively administered with two intramuscular injections of LNP at above-mentioned three doses on Day 0 and Day 21 (simulating the clinical schedule of BNT162b2). Subsequently, serum samples were collected at 12 designated time points (Day 0, 3, 5, 7, 14, 21, 24, 26, 28, 35, 42 and 49) and examined for the presence and level of anti-PEG IgM with ELISA. The obtained data were summarized in Fig. 3B,

with statistical analysis conducted among control, L-LNP, M-LNP and H-LNP groups for each time point.

Our data indicated that anti-PEG IgM was initially detected in L-LNP group on Day 3 after the first injection. Impressively, although the serum anti-PEG IgM was not detectable until Day 5 after the first injection of M-LNP and H-LNP, the initial antibody levels induced by these two LNP doses were significantly higher than that induced by L-LNP ($P < 0.001$, L-LNP *vs* M-LNP; $P < 0.0001$, L-LNP *vs* H-LNP). Another finding is that during the first injection cycle (Day 0~21), L-LNP transiently induced anti-PEG IgM only detectable on Day 3 and Day 5, while M-LNP and H-LNP induced more persistent and higher levels of anti-PEG IgM detectable on Day 5, 7, 14 and 21. These data suggest that an initial single injection of PEGylated LNP induced both time- and dose-dependent induction of anti-PEG IgM. Interestingly, anti-PEG IgM was detected at more time points for all LNP doses after the second injection. For instance, there were 4 anti-PEG IgM-detectable time points (Day 24, 26, 28 and 35) in LNP group after the second injection, while there were only 2 anti-PEG IgM-detectable time points (Day 3 and Day 5) during the first injection cycle. M-LNP and H-LNP even constantly induced anti-PEG IgM throughout the whole second injection cycle (Day 21~42) and the extension period (Day 42~49). In addition, there was statistical significance among different groups/doses on the level of anti-PEG IgM, which was ranked as follows: H-LNP > M-LNP > L-LNP at all detectable time points including Day 24, 26, 28 and 35. These data provided additional evidence for the dose- and time-dependency of anti-PEG IgM induced by PEGylated LNP. Further calculation and comparison showed that the peak levels of anti-PEG IgM induced by the second injection of LNP were higher than those induced by the first injection at the same dose: L-LNP, 2.374 on Day 28 *vs* 1.996 on Day 5; M-LNP, 3.692 on Day 26 *vs* 2.704 on Day 5; H-LNP, 4.262 on Day 26 *vs* 2.492 on Day 5. Herein, we would like to emphasize that the high ELISA assay precision, as indicated by the very low variation of standards (CV% = 3.365 ± 2.934%) and samples (CV% = 4.342 ± 5.510%), as well as the high average linear regression coefficient of determination of standard curves ($R^2 = 0.985 \pm 0.005$), demonstrated that our ELISA assays for anti-PEG IgM had good quality control and the obtained data were reliable (Fig. 3C).

As indicated by plotted curves (Fig. 3D), profile analysis found that time-courses of anti-PEG IgM production between every two groups showed different profiles. Furthermore, changes over time (12 time points) and differences across groups (3 doses) regarding LNP-induced anti-PEG IgM were evaluated for statistical significance using linear mixed model analysis. As indicated by corresponding statistical analysis (Table 1), β for "Group", which represented differences on antibody level among various groups at all time points, exhibited statistical significance between Control *vs* M-LNP ($P < 0.0001$), Control *vs* H-LNP ($P = 0.0035$) and L-LNP *vs* M-LNP ($P = 0.0011$). Significant differences were also detected with β for "Time" ($P = 0.0116$) and "Time^2" ($P < 0.0001$), both of which represent rate of change in antibody level over time (12 time points). Regarding β for "Group*Time", which represented mean differences in the rate of change in antibody level over time among various groups, we found that compared with the Control

group, both M-LNP and H-LNP groups had faster rates of anti-PEG IgM production (β for M-LNP*Time: 0.0238 [0.0167, 0.0308] higher per day, β for H-LNP*Time: 0.0458 [0.0387, 0.0528] higher per day, both $P < 0.0001$ *vs* Control*Time), while the change rate of L-LNP group was similar to the Control group (β for L-LNP*Time: 0.0034 [-0.0036, 0.0105] higher per day, $P = 0.3408$ *vs* Control*Time). Particularly, H-LNP group exhibited the fastest rate in anti-PEG IgM production among the four groups (H-LNP*Time *vs* L-LNP*Time, H-LNP*Time *vs* M-LNP*Time, M-LNP*Time *vs* L-LNP*Time, all $P < 0.0001$). These data have provided additional evidence for dose- and time- dependent induction of anti-PEG IgM by PEGylated LNP. Another interesting finding discovered by linear mixed model analysis was the significant difference on antibody level between the first and second injections (β for "Second Injection": 0.9166 [0.7852, 1.0479], $P < 0.0001$ *vs* First Injection), which coincides with the longer lasting period and higher level of anti-PEG IgM induced by repeated injection of LNP compared with the initial injection (Fig.3, B and D).

Time- and dose-dependent induction of anti-PEG IgG antibody by PEGylated LNP

Serum samples collected at above-mentioned 12 time points were further examined for the presence and level of anti-PEG IgG with ELISA. The obtained data were summarized in Fig. 4A, with a high ELISA assay precision demonstrated by the very low variation of standards (CV%=3.472 ± 3.634%) and samples (CV%=4.545 ± 7.867), as well as the high average linear regression coefficient of determination of standard curves (R^2=0.999 ± 0.001) (Fig. 4B). Different from the characteristics of LNP in inducing anti-PEG IgM (Fig. 3), no anti-PEG IgG was detected throughout the first injection cycle in all experimental groups (Day 0~21). These data demonstrate that an initial single injection of PEGylated LNP, at a broad range of doses tested in this study, did not induce anti-PEG IgG antibody in Wistar rats. Interestingly, although anti-PEG IgG was still not detectable after the second injection of L-LNP (Day 21~49), it was clearly induced by a repeated injection of M-LNP and H-LNP, and constantly existed at all later time points tested (Day 24~49). Similar to the findings with anti-PEG IgM, anti-PEG IgG levels induced by H-LNP were significantly higher than those induced by M-LNP at all detectable time points, demonstrating a dose-dependency on anti-PEG IgG induced by PEGylated LNP. In particular, the anti-PEG IgG levels increased to the peaks on Day 26 in both M-LNP and H-LNP groups (2.083 ± 0.306 and 2.547 ± 0.247, respectively, Fig. 4, A and C). Another point worthy of note is that anti-PEG IgM levels induced by LNP were generally higher than the corresponding values of anti-PEG IgG.

As indicated by plotted curves (Fig. 3C), profile analysis found that time-courses of anti-PEG IgG production in the control and L-LNP groups had equal levels whereas other comparisons of time-courses between every two groups showed different profiles. Linear mixed model analysis was further conducted to evaluate the statistical significance on changes of LNP-induced anti-PEG IgG over time (12 time points) and differences across groups (3 doses). As indicated by corresponding statistical analysis (Table 2), β for "Group", which represented differences on antibody level among various groups at all time points, exhibited statistical significance between

M-LNP *vs* L-LNP ($P = 0.0195$), H-LNP *vs* L-LNP ($P = 0.0054$). Significant differences were also detected with β for "Time" ($P = 0.0077$) and "Time^2" ($P = 0.0197$), both of which represent rate of change in antibody level over time (12 time points). Regarding β for "Group*Time", which represented mean differences in the rate of change in antibody level over time among various groups, we found that compared with the Control group, both M-LNP and H-LNP groups had faster rates of anti-PEG IgG production (β for M-LNP*Time: 0.0149 [0.0105, 0.0193] higher per day, β for H-LNP*Time: 0.0244 [0.0200, 0.0288] higher per day, both $P < 0.0001$ *vs* Control*Time), while the change rate of L-LNP group was similar to the Control group (β for L-LNP*Time: 0.0011 [-0.0033, 0.0054] higher per day, $P = 0.6339$ *vs* Control*Time). Particularly, H-LNP group exhibited the fastest rate in anti-PEG IgG production among the four groups (H-LNP*Time *vs* L-LNP*Time, H-LNP*Time *vs* M-LNP*Time, M-LNP*Time *vs* L-LNP*Time, all $P < 0.0001$). These data have provided additional evidence for dose- and time- dependent induction of anti-PEG IgG by PEGylated LNP. Another interesting finding discovered by linear mixed model analysis was the significant difference on antibody level between the first and second injections (β for "Second Injection": 0.6549 [0.5734, 0.7364], $P < 0.0001$ *vs* First Injection) (Fig.4, A and C).

Enhanced production of anti-PEG antibodies by previous exposure to PEGylated LNP

To evaluate the potential influence of previous exposure to PEGylated LNP on the production of anti-PEG IgM and IgG antibodies after subsequent exposure to same LNP, increased anti-PEG IgM (▲Anti-PEG IgM (Log_{10} CONC)) and increased anti-PEG IgG production (▲Anti-PEG IgG (Log_{10} CONC)) were respectively calculated by subtracting log10-transformed anti-PEG antibody concentration determined by quantitative ELISA assay after first injection (Anti-PEG IgM (Log_{10} $CONC_{1st\ injection}$) or Anti-PEG IgG (Log_{10} $CONC_{1st\ injection}$)) from log10-transformed antibody concentration determined after the second injection (Anti-PEG IgM (Log_{10} $CONC_{2nd\ injection}$) or Anti-PEG IgG (Log_{10} $CONC_{2nd\ injection}$)) at corresponding 3 doses and 6 time points (Day 0, 3, 5, 7, 14 and 21). The obtained data were summarized in Fig. 5 (A and B for ▲Anti-PEG IgM (Log_{10} CONC), C and D for ▲Anti-PEG IgG (Log_{10} CONC)). As introduced in Fig. 5B, profile analysis found that time-courses of enhanced anti-PEG IgM production (▲Anti-PEG IgM (Log10 CONC)) between every two groups showed different profiles.

As indicated in Fig. 5A, although ▲Anti-PEG IgM (Log_{10} CONC) was not detectable until Day 5 in L-LNP group, increased anti-PEG IgM production was observed at all the time points in both M-LNP and H-LNP groups. Moreover, two sequential injections of L-LNP only induced transient ▲Anti-PEG IgM (Log_{10} CONC) detectable on Day 5, 7 and 14, while those of M-LNP and L-LNP induced more persistent and higher level of ▲Anti-PEG IgM (Log_{10} CONC) detectable on Day 3, 5, 7, 14 and 21. In particular, the peak levels of ▲Anti-PEG IgM (Log_{10} CONC) induced by different doses of PEGylated LNP were 0.654 ± 0.471 (L-LNP, Day 7), 1.574 ± 0.399 (M-LNP, Day 3) and 2.277 ± 0.410 (H-LNP, Day 3), respectively (Fig. 5, A and B). Importantly, by using linear mixed model analysis, we further demonstrated the statistical significance on changes over 6 time points and differences across groups (3 doses) regarding LNP-induced ▲Anti-PEG IgM

(Log_{10} CONC) (Fig. 5, A and B; Table 3). For instance, the dose dependency of enhanced production of anti-PEG IgM was confirmed, as ▲Anti-PEG IgM (Log_{10} CONC) ranking from high to low was that respectively induced by H-LNP, M-LNP and L-LNP at all detectable time points, with significant difference among these three groups ($P < 0.0001$ for M-LNP *vs* L-LNP and H-LNP vs L-LNP; $P = 0.0003$ for H-LNP *vs* M-LNP). Moreover, rate of change in ▲Anti-PEG IgM (Log_{10} CONC) over 6 time points also exhibited significant differences, with $P < 0.0001$ for both "Time" and "$Time^2$". Regarding β for "Group*Time", which represented mean differences in the rate of change in ▲Anti-PEG IgM (Log_{10} CONC) over time among various groups, we found that compared with the L-LNP group, both M-LNP and H-LNP groups had faster rates of ▲Anti-PEG IgM (Log_{10} CONC) ($P = 0.0138$, M-LNP*Time *vs* L-LNP*Time; $P = 0.0149$, H-LNP*Time *vs* L-LNP*Time). These data have provided additional evidence for dose- and time- dependency of ▲Anti-PEG IgM (Log_{10} CONC) induced by two sequential injections of PEGylated LNP.

Furthermore, quantification of increased anti-PEG IgG production (▲Anti-PEG IgG (Log_{10} CONC)) was summarized in Fig. 5C, with time-course profiles of ▲Anti-PEG IgG (Log_{10} CONC) across four groups plotted in Fig. 5D and linear mixed model analysis summarized in Table 4. As introduced in Fig. 5D, profile analysis found that time-courses of enhanced anti-PEG IgG production (▲Anti-PEG IgG (Log10 CONC)) in the control and L-LNP groups were also equivalent whereas other comparisons of time-courses between every two groups showed different profiles. Our data showed that ▲Anti-PEG IgG (Log_{10} CONC) was not detectable in L-LNP group at all time points. Nor was it detectable on Day 0 of L-LNP, M-LNP or H-LNP groups. However, ▲Anti-PEG IgG (Log_{10} CONC) was detected at all later time points (Day 3, 5, 7, 14 and 21) in both M-LNP and H-LNP groups, with peak levels induced on Day 5 (0.888 ± 0.459) and Day 7 (1.354 ± 0.308), respectively (Fig. 5, A and B). Moreover, statistical significance was observed between various groups including Control *vs* M-LNP, Control *vs* H-LNP, L-LNP *vs* M-LNP, L-LNP *vs* H-LNP and M-LNP *vs* H-LNP. Consistent with these data, Control and L-LNP groups exhibited quite similar time-course profile of ▲Anti-PEG IgG (Log_{10} CONC), whereas there was significant difference among profiles of Control/L-LNP, M-LNP and H-LNP groups (Fig. 5B). Indeed, data introduced in Table 4 further confirmed these findings, as ▲Anti-PEG IgG (Log_{10} CONC) ranking from high to low was that respectively induced by H-LNP, M-LNP and L-LNP at all detectable time points, with significant difference among these three groups (β for L-LNP: 0.0149 [-0.1866, 0.2164], β for M-LNP: 0.5180 [0.3165, 0.7195]; β for H-LNP: 0.8861 [0.6846, 1.0876]; $P < 0.0001$, comparisons between any two groups). Together with the significant differences on rate of change in ▲Anti-PEG IgG (Log_{10} CONC) over 6 time points ($P < 0.0001$ for both "Time" and "$Time^2$"), our data clearly demonstrated that initial injection of PEGylated LNP dose- and time-dependently boosted the generation of anti-PEG IgM and IgG after the second injection.

Biodistribution of PEGylated LNP administered at three clinically relevant doses simulating clinical schedule.

By using a fluorescence/bioluminescence double-labeled LNP (DiR-LU@LNP), the

biodistribution of PEGylated LNP was determined in Wistar rats administered with two intramuscular injections of DiR-LU@LNP at above-mentioned three doses and with a 21-day interval (Fig. 6A and "Methods"). Six hours after each injection, a series of primary organs or tissues including muscle at the injection site, liver, spleen, lung, kidney, heart and draining lymph were isolated and examined for their fluorescence and bioluminescence with IVIS Spectrum imaging system. As shown in fig. S4, consistent with the biodistribution data reported by Pfizer *Inc.* in both mice and rats (assessment report of Comirnaty®/BNT162b2, issued by the European Medicines Agency), weak bioluminescence signal of firefly luciferase was detected in muscle at injection site and liver, which demonstrates that DiR-LU@LNP effectively delivered active luciferase mRNA and drained into the liver, leading to expression of luciferase protein. Notably, in our newly synthesized DiR-LU@LNP, DiR fluorescence exhibited significantly higher sensitivity than firefly luciferase bioluminescence in labeling LNP (fig. S4 and Fig. 6B). Therefore, the biodistribution of LNP was determined and analyzed based on DiR fluorescence in this study.

As shown in Fig. 6B, 6 hours after both the first and second injections, DiR fluorescence was only detectable in muscle at the injection site in rats administered with low dose of DiR-LU@LNP (L-LNP group). When the dose of DiR-LU increased to middle dose (M-LNP group), the fluorescent signal was significantly increased and could be observed in muscle at the injection site, liver and lung. As expected, the fluorescent signal was further enhanced and accumulated in multiple organs including muscle at the injection site, liver, lung, spleen and draining lymph node in the H-LNP group. These findings clearly demonstrate a dose-dependent biodistribution of LNP, with preferential accumulation in reticuloendothelial system such as liver, lung, spleen and draining lymph node after entering the blood circulation *via* intramuscular injection (Fig. 6C). Further normalization through dividing the total radiant efficiency (TRE) by the mass of corresponding organ and subsequent analysis revealed that there was no statistical difference on LNP-associated fluorescence intensity between two injections in all DiR-detectable organs (Fig. 6D and fig. S5), suggesting that the first injection of PEGylated LNP did not exhibit significant influence on the biodistribution of the same LNP injected 21 days later at the same dose.

Blood clearance of PEGylated LNP administered at three clinically relevant doses simulating clinical schedule

To explore whether previous exposure to PEGylated LNP would alter the pharmacokinetic of newly or repeatedly injected LNP, Wistar rats were administered with two intramuscular injections with DiR-labeled LNP (DiR-LNP) at above-mentioned doses and schedule (Fig. 7A and "Methods"). After each injection, serum samples were respectively collected at a series of designated time points including 5 minutes, 30 minutes, 1 hour, 3 hours, 6 hours, 10 hours, 24 hours and 48 hours for further measurement of DiR fluorescence intensity with a SpectraMax® iD5 multi-mode microplate reader. As shown in Fig. 7B, LNP-associated DiR fluorescence was not detectable in serums collected from L-LNP group at all time points after both injections, indicating the extremely low level of LNP in blood circulation of rats administered with low dose of DiR-LNP.

However, significantly increased DiR fluorescence was observed in serums isolated from M-LNP (at 6 hours and 10 hours) and H-LNP (at 7 sequential time points ranging from 30 minutes till 48 hours) groups after an initial exposure to DiR-LNP. These data coincide with the above-mentioned dose-dependent induction of anti-PEG antibodies by LNP administered at same clinically relevant doses simulating clinical schedule. Interestingly, compared with the first injection, DiR fluorescence was detected at less time points in M-LNP (only 6 hours) and H-LNP (4 sequential time points ranging from 6 hours till 48 hours) groups after the second injection of DiR-LNP, suggesting faster blood clearance and/or reduced serum level of PEGylated LNP upon repeated exposures. Indeed, as depicted in Fig. 7C and Fig. 7D, although no statistical difference on LNP-associated fluorescence intensity was observed between two separate injections in Control, L-LNP and M-LNP groups, DiR fluorescence was significantly decreased at 30 minutes ($P < 0.01$), 1 hour ($P < 0.05$) and 48 hours ($P < 0.05$) after repeated injection of high-dose DiR-LNP in comparison with that after the initial injection. For the first time, these data demonstrate an accelerated blood clearance phenomenon of clinically relevant PEGylated LNP triggered by previous exposure to the same LNP.

Discussion

PEG is a versatile polymer commonly used as a surfactant, solvent and emulsifying agent in household chemicals, as an additive in foods, and as either an active composition or an inactive excipient in medicine (*27*). Taking the multiple advantages of modifying therapeutics with PEG (PEGylation), FDA has approved 33 PEGylated agents for a variety of clinical indications such as metabolic disease, immunological disease, degenerative disease, cancer and infectious diseases (https://www.drugs.com). Although free PEG is poorly immunogenic and doesn't effectively elicit anti-PEG antibody response, it may acquire immunogenic properties, e.g. inducing anti-PEG antibodies, upon conjugation with other materials such as proteins and nanocarriers *(27, 28)*. Therefore, PEG is considered to be a polyvalent hapten (*28*). Interestingly, a proportion of individuals who never received PEGylated drugs have anti-PEG antibodies due to environmental exposure (*8*). For instance, an epidemiological study based on 1504 healthy Han Chinese donors residing in Taiwan area of China found that a total of 666 individuals (44.3%) had positive anti-PEG IgG or IgM, with 25.7%, 27.1%, and 8.4% of the total population having anti-PEG IgG only, anti-PEG IgM only, and both anti-PEG IgG and IgM, respectively (*29*). This study also showed that PEG-specific antibodies were more common in females than in males (32.0% vs 22.2% for IgM and 28.3% vs 23.0% for IgG), and in young people (up to 60% for 20 years old) as compared to old people (20% for >50 years old). Another epidemiological study based on 377 healthy human blood donors in USA found that anti-PEG antibodies were detectable in ~72% of individuals, with 18%, 25% and 30% of all samples having anti-PEG IgG only, anti-PEG IgM only, and both anti-PEG IgG and IgM, respectively (*30*). Importantly, anti-PEG antibodies could form "antigen-antibody" complexes with newly administered PEGylated nanocarriers/proteins, leading to biodistribution/pharmacokinetic changes of PEGylated drugs and reduced therapeutic efficacy (*8,*

27). Moreover, they may induce severe side effects such as hypersensitivity reactions of PEGylated therapeutics, although the underlying mechanisms have not been fully clarified (*27, 31*).

In the past five years, three PEGylated LNP-delivered drugs have been marketed, including Patisiran, BNT162b2 and mRNA-1273. As the first two vaccines using PEG as an excipient and/or using LNP as a carrier, BNT162b2 and mRNA-1273 essentially represent a new class of vaccines, because their biodistribution and pharmacokinetics are mainly determined by the characteristics of their nanocarrier, e.g. the PEGylated LNP prepared in this study. Unfortunately, in spite of these significant differences from traditional vaccines, no pharmacokinetic data are available for either PEGylated LNP or two LNP-delivered mRNA vaccines, as currently these data are not regularly required by WHO for market approval of intramuscular vaccines (*32*). Considering that the worldwide sales volume of BNT162b2 and mRNA-1273 has respectively reached as huge as >5,341,276,760 and >3,229,743,423 doses (public information from WHO), it is urgent to reveal the properties of PEGylated LNP in inducing PEG-related immunological effects, e.g. production of PEG-specific antibodies and subsequent influence on the pharmacokinetic of newly/repeatedly injected LNP, as these characteristics may directly affect the immune protective efficacy of both vaccines. Furthermore, clarification of these issues will provide valuable information for the research and development of a number of vaccine candidates using PEGylated LNP as a carrier (public information from WHO).

Up to date there are four published clinical investigations in total that evaluated the induction of PEG-specific antibodies by LNP-delivered drugs, including three related with BNT162b2, mRNA-1273 and mixed use of these two vaccines (*16-19*). Unfortunately, it is extremely and practically difficult to obtain reliable data with clinical studies. One major reason is the significant variability of pre-existing PEG-specific antibodies, leading to unfavorable intervention when identifying and analyzing antibodies induced by PEGylated LNP. Alnylam Pharmaceuticals Inc. reported that only two of 224 patients (0.89%) with hereditary transthyretin-mediated (hATTR) amyloidosis were positive for anti-PEG antibodies at baseline (*16*), while Kent et al from the University of Melbourne stated that anti-PEG IgG was commonly detectable (71%) before vaccination in BNT162b2 and mRNA-1273 cohorts (*17*). Calzolai et al from Joint Research Centre in Italy described that anti-PEG IgG was positive before the first vaccine injection in their cohorts receiving two LNP-based COVID-19 vaccines, with a large person-to-person variability (*18*). Another big concern is that additional exposure to PEG derivatives other than PEGylated LNP may exist during clinical observation period, which may interfere with the immunological effects induced by injected LNP. In agreement with this concern, Kent et al showed that 5 unvaccinated control donors had increased level of anti-PEG IgG, and 8 control donors had elevated anti-PEG IgM (*17*). Moreover, insufficient/very small population size, broad age range, gender-related influence, significant deviation of time points even within the same cohort, and crosstalk between BNT162b2 and mRNA-1273 upon mixed use, were additional shortcomings commonly existed in related literatures. As a result, till now no consistent evidence has been obtained regarding any characteristic of initial and/or repeated injections of either BNT162b2 or mRNA-1273 in inducing

PEG-specific antibodies. Besides, the fold changes of both anti-PEG IgM and IgG induced by either mRNA vaccine had a very broad range, further demonstrating the remarkable person-to-person variability in clinical studies.

In order to clarify the cause-and-effect relationships of clinically relevant PEGylated LNP on the induction of PEG-associated immunological effects, we herein initiated the first animal study by using the PEGylated LNP of BNT162b2, which has the largest number of recipients all over the world, and simulating its clinical practice as a representative model system. As expected, neither anti-PEG IgM (Fig. 3, B and D) nor anti-PEG IgG (Fig. 4, A and C) was detected in all experimental groups on Day 0 before initial injection of PEGylated LNP. Nor did any type of anti-PEG antibodies exist in control group throughout the whole study period (Day 0-49) (Fig. 3, B and D; Fig. 4, A and C). These data demonstrate a "clean" background and no additional "cause" other than injected LNP in our model system. Meanwhile, the shortcomings existed in clinical studies, e.g. insufficient group size, deviations on time points, as well as age- and gender-associated interferences, were easily resolved in this study. Encouragingly, through designing a series of time points and three doses respectively correlated with the amount of PEG contained in three LNP-based drugs in market (Fig. 3A), we carefully investigated the potential time- and dose-dependency of clinically relevant LNP in inducing anti-PEG antibodies. Our data clearly demonstrated that generation and changes of both anti-PEG IgM (Fig. 3, B and D; Table 1) and anti-PEG IgG (Fig. 4, A and C; Table 2) were time-dependent. In brief, anti-PEG IgM emerged on Day 3, reached the peak level on Day 5 and then gradually reduced during the first injection cycle (Day 0~21), followed by a further boosted peak on Day 26-28 after the second injection of LNP on Day 21 (Fig. 3, B and D; Fig. 5, A and B). Despite of the absence throughout the first injection cycle (Day 0~21), anti-PEG IgG emerged on Day 24 after the second injection of LNP on Day 21, and reached its peak on Day 26 (Fig. 4, A and C; Fig. 5, C and D). Meanwhile, utilization of three doses (1:38:262) essentially simulating the corresponding amount of PEG contained in a single injection of BNT162b2, mRNA-1273 and Patisiran revealed the dose dependency of LNP in inducing anti-PEG antibodies. Specifically, the amount of PEGylated LNP injected was positively correlated with the generation and serum level of anti-PEG antibodies (Fig. 3D and Fig. 4C).

Further investigation on the biodistribution of PEGylated LNP demonstrated that in addition to muscle at the injection site, LNP mainly accumulated in reticuloendothelial system such as liver, lung, spleen and draining lymph node (Fig. 6, B and C), which is essentially consistent with the biodistribution data described in the Public Assessment Report of BNT162b2 and mRNA-1273 (*33,34*). Importantly, we discovered that initial injection of LNP promoted the blood clearance of subsequently administered LNP (Fig. 7, C and D; fig. S5). To our best knowledge, this is the first study on the pharmacokinetics of two LNP-based COVID-19 vaccines or their PEGylated LNP carriers. It is noteworthy that although previously Alnylam Pharmaceuticals Inc. reported that ABC phenomenon was absent after repeated injection of Onpattro, all patients with hATTR amyloidosis in their study received corticosteroid premedication prior to each Onpattro injection to reduce the risk of infusion-related reactions (*16*). However, corticosteroid is generally considered as an

immunosuppressive drug and may repress PEG-associated immunological effects including "antigen-antibody" immune complex-mediated ABC phenomenon. Our findings on the ABC phenomenon of PEGylated LNP, together with further in-depth pharmacokinetic studies on LNP or LNP-based therapeutics, may lead to optimization of the guidelines/premarket requirements for research and development of biomedical products using PEGylated LNP as delivery vectors. For instance, preclinical pharmacokinetic studies might be necessary and important before market approval of vaccines or other drugs delivered intramuscularly using LNP.

Finally, our model system has provided an opportunity to explore the mechanisms mediating the generation of anti-PEG antibodies induced by clinically relevant PEGylated LNP (fig. S6). It is well known that non-protein antigens, such as lipids, polysaccharides, and naturally occurring non-proteinatious and synthetic polymers, can stimulate antibody response in the absence of T helper cell and is therefore called thymus-independent antigens or T cell-independent antigens (TI-Ag) (*8, 31*). In contrast, T-dependent antigens (TD-Ag) mainly include proteins/peptides that are uptaken by the antigen-presenting cells and presented in the context with major histo-compatibility complex type 2 (MHC II) to the T helper lymphocytes (*8, 31*). According to its chemical nature, PEGylated LNP is similar to PEGylated liposome and belongs to TI-Ag, as it doesn't contain any proteinatious composition. Traditionally, there has been a perception that TI-Ag could not induce isotype switch from IgM to long-lasting IgG, resulting in the production of IgM only (no or very low level of IgG) after administration of TI-Ag. Moreover, it is generally believed that TI-Ag is not able to induce a typical recall antibody response, which is also called immunological memory or B cell memory characterized by an amplified, accelerated and affinity-matured antibody production after successive exposure to certain antigens such as TD-Ag (*31-36*). Consistent with these theories, even six repeated injections of PEGylated liposome (with a seven-day interval) did not enhance the anti-PEG IgM production in mice, and the anti-PEG IgG level remained extremely low throughout the study (*37*). Interestingly, after a thorough literature search, we found that although three types of TI-Ag, including B. hermsii (Borrelia hermsii, a relapsing fever bacterium), NP-Ficoll (4-hydroxy-3-nitrophenylacetyl-Ficoll, a model TI-Ag) and pneumococcal capsular PS3 (serotype 3 capsular polysaccharide), could induce immune memory (*38-40*), previously there is no report on either inducing immune memory or isotype switching from IgM to IgG by any PEG derivatives belonging to TI-Ag. Herein, unexpectedly we discovered that different from other PEG derivatives which belong to TI-Ag such as PEGylated liposome, PEGylated LNP could not only induce isotype switch and subsequent production of anti-PEG IgG (Fig. 4, A and C), but cause immune memory/B cell memory, leading to rapid enhancement and longer lasting time of both anti-PEG IgM and IgG upon repeated injection (Fig. 5, Table 3 and Table 4). These findings will refresh our understandings and break our traditional expectations on PEGylated LNP, and possible other PEG derivatives belonging to TI-Ag.

Materials and Methods

Materials

Cholesterol and 1,2-distearoyl-snglycero-3-phosphocholine (DSPC) were purchased from Lipoid GMBH (Ludwigshafen, Germany). ((4-hydroxybutyl)azanediyl)bis(hexane-6,1-diyl)bis(2-hexyldecanoate) (ALC-0315) and 2-[(polyethylene glycol)-2000]-N,N-ditetradecylacetamide (ALC-0159) were acquired from SINOPEG (Xiamen, China). Ferric chloride hexahydrate, ammonium thiocyanate and polyethylene glycols (PEG10000) were obtained from Sigma-Aldrich (St. Louis, MO, USA). 3-[(3-cholamidopropyl)dimethylammonio]-1-propanesulfonate (CHAPS), 3,3′,5,5′-Tetramethylbenzidine dihydrochloride hydrate (TMB 2HCl) and nonfat powdered milk were purchased from Beyotime Biotechnology (Shanghai, China). Maxisorp 96-well microplates was acquired from Nalge-Nunc International (Rochester, NY, USA). D-Luciferin were purchased from Thermo Fisher Scientific (Waltham, MA, USA). Firefly luciferase mRNA was obtained from Trilink Biotechnologies (San Diego, California, USA). Rat anti-PEG IgM (rAGP6) and rat anti-PEG IgG (r33G) were acquired from Academia Sinica (Taipei, China). Peroxidase-conjugated affinipure rabbit anti-rat IgM μ-chain specific and peroxidase-conjugated affinipure donkey anti-rat IgG (H+L) were obtained from Jackson ImmunoResearch Laboratories Inc (West Grove, PA, USA).

Preparation of LNP, DiR-LNP and DiR-LU@LNP

LNP, DiR-LNP and DiR-LU@LNP were formulated using a modified procedure previously described (*27*). First, the ethanol phase was prepared by dissolving ALC-0315, DSPC, cholesterol and ALC-0159 at a molar ratio of 46.3: 9.4: 42.7: 1.6, respectively. For preparing DiR-LNP and DiR-LU@LNP, DiR was added into the lipids in ethanol at 0.4% mol. For preparing LNP and DiR-LNP, the aqueous phase was prepared using 20 mM citrate buffer (pH4.0). For preparing DiR-LU@LNP, the aqueous phase was prepared using 20 mM citrate buffer (pH4.0) containing firefly luciferase mRNA. Then, the ethanol phase was combined with the aqueous phase at a flow rate ratio of 1: 3 (ethanol: aqueous) through a microfluidic mixer (Precision Nanosystems Inc., Canada). Following microfluidic mixing, nanoparticle solutions were dialyzed against 10×volume of PBS (pH7.4) through a tangential-flow filtratio (TFF) membrane with 100 kD molecular weight cut-offs (Sartorius Stedim Biotech) for at least 18 h. Next, nanoparticle solutions were concentrated using Amicon ultra-centrifugal filters (EMD Millipore, Billerica, MA, USA), passed through a 0.22 μm filter, and stored at 2~8°C until use.

Characterization of LNP, DiR-LNP and DiR-LU@LNP

LNP, DiR-LNP and DiR-LU@LNP were examined for their hydrodynamic size (Z-average), polydispersity index (PDI) and zeta potential with dynamic light scattering (Zetasizer Nano ZS, Malvern Instruments Ltd, Malvern, UK) equipped with a solid state HeNe laser (λ = 633 nm) at a scattering angle of 173˚. For Z-average and PDI measurements, nanoparticles were added in PBS (pH7.4). For zeta potential measurements, nanoparticles were added in ultrapure water. The samples were tested at 25˚C for 10 s (pre-equilibration for 2 min) and repeated at least 10 times in 4-mL disposable cuvettes (for Z-average and PDI) or zeta cuvettes (for zeta potential). Samples were

analysed in triplicate and reported as the mean ± standard deviation.

The morphological characteristics of LNP, DiR-LNP and DiR-LU@LNP were observed with cryogenic transmission electron microscopy (Cryo-TEM). All samples (3 μL) were deposited on a holey carbon grid that was glow-discharged (Quantifoil R1.2/1.3) and vitrificated using a Vitrobot Mark IV System (FEI/Thermo Scientific). Cryo-TEM imaging was performed on a Talos F200C device (FEI/Thermo Scientific) equipped with a Ceta 4k x 4k camera at 200 kV accelerating voltage in the Center of Cryo-Electron Microscopy, Zhejiang University.

The final phospholipid (DSPC) concentrations of LNP, DiR-LNP and DiR-LU@LNP solutions were quantified via Steward's assay to calculate their administered doses in animal experiments (*42*). Briefly, a ferrothiocyanate reagent was prepared with 27.03 mg ferric chloride hexahydrate and 30.4 mg ammonium thiocyanate dissolved in 1 mL of distilled water. A volume of 10 μL of the lipid sample was added to 990 μL of chloroform, followed by addition of 1 mL of ammonium ferrothiocynate reagent. The mixture was vortexed for 60 seconds and then centrifuged at 1000 rpm for 15 minutes at RT. The chloroform layer was transferred to a glass cuvette and the absorbance was measured at 470 nm using a Unicam UV500 Spectrophotometer (Thermo electron corporation, USA). Calibration curves for DSPC lipids of 25–150 μg/mL were obtained and used to calculate the final phospholipid (DSPC) concentrations of LNP, DiR-LNP and DiR-LU@LNP solutions.

To assess their stability in serum, LNP, DiR-LNP and DiR-LU@LNP were diluted 100-fold with PBS containing 10% rat serum and then incubated at 37℃ for 24 h. Subsequently, 1 mL of dilutions of LNP, DiR-LNP and DiR-LU@LNP were collected at designated time points (1, 6, 12, 24 h post-incubation), followed by characterization of Z-average and PDI with DLS. All samples were measured in triplicate. Data are represented as the mean ± standard deviation.

Calculation and determination of LNP dosing protocols

1) Calculation of mPEG2000 exposure amount of three FDA-approved LNP-delivered therapeutics (using 60 kg as the reference body weight of an adult)

I. BNT162b2: The mPEG2000 exposure with one dose of BNT162b2 is approximately 0.0406 mg (*21*). Correspondingly, the exposure of phospholipid (DSPC) is 0.09 mg based on the formula of the BNT162b2.

II. mRNA-1273: Although the total lipids content is 1.93 mg per dose, we do not know the accurate mPEG2000-DMG content (*22*). Assuming a content of 1.93 mg of mPEG2000-DMG, the content of mPEG2000 is calculated to be 1.5385 mg, which is 38 times that of BNT162b2.

III. ONPATTRO (Patisiran): Patisiran is the active siRNA component of ONPATTRO, its clinical preparation concentration is 2 mg/mL and its clinical dose was 0.3 mg patisiran/kg. Therefore, adults need to inject 9 mL of ONPATTRO each time. The exposure of mPEG2000 is approximately 10.6434 mg. which is 262 times that of BNT162b2 (*20*).

2) Conversion of human doses to rat equivalent doses and determination of three clinically relevant LNP doses (using 60 kg as the reference body weight of an adult)

According to the experimental animal-human dose exchange algorithm (animal equivalent

dose (mg/kg) = human dose (mg/kg) × K_m ratio (K_m ratio of rat is 6.2)) (*43*), the dose of LNP in rats equivalent to that in each single injection of BNT162b2 in adults was calculated as follows: 0.09 mg/60 kg × 6.2 = 0.009 mg phospholipid /kg. Similarly, the LNP dose in rats equivalent to that in each single injection of mRNA-1273 in adults was calculated as: 0.009 × 38 = 0.342 mg phospholipids /kg; the rat LNP dose equivalent to that in each single injection of ONPATTRO in adults was calculated as: 0.009 × 262 = 2.358 mg phospholipids/kg. Therefore, the above three clinically relevant LNP doses were used in this study: low dose (L-LNP, 0.009 mg phospholipids/kg), middle dose (M-LNP, 0.342 mg phospholipids/kg) and high dose (H-LNP, 2.358 mg phospholipids/kg).

3) Determination of LNP administration route, frequency and interval

The clinical administration route of BNT162b2 is intramuscular injection, once every 3 weeks (routine vaccination twice). Therefore, we essentially simulated the clinical protocols of BNT162b2 in this study (intramuscular injection twice with a 3 week-interval).

Animals

10-12-week-old female Wistar rats were purchased through the Laboratory Animal Center of Zhejiang University and housed under controlled environmental conditions at constant temperature, humidity, and a 12-h dark-light cycle in the animal center. Rats were given ad libitum access to a standard rat chow and water, and were acclimated for at least 7 days. All animal experiments were approved by the Laboratory Animal Welfare and Ethnics Committee of Zhejiang University and carried out in accordance with the guidelines of the committee (approval No. ZJU20210071).

Administration of PEGylated LNP simulating clinical application

Wistar rats were randomly divided into a control group (n=8) and three experimental groups (n=15). At Day 0, experiment group 1 (L-LNP group) was intramuscularly injected with 0.009 mg phospholipids/kg LNP; experiment group 2 (M-LNP group) was intramuscularly injected with 0.342 mg phospholipids/kg LNP; experiment group 3 (H-LNP group) was intramuscularly injected with 2.358 mg phospholipids/kg LNP; control group only received PBS as a placebo control. At Day 21, each group was boosted intramuscularly with a dose of LNP equivalent to initial injection. All experiments were performed using standard administration techniques. Peripheral blood was collected from the retro-orbital venous plexus at Day 0, 3, 5, 7, 14, 21, 24, 26, 28, 35, 42 and 49. Blood was centrifuged at 2000×g and 4 °C for 15 minutes, and the serum was immediately stored at -80 °C for quantification of anti-PEG antibody.

Quantification of anti-PEG IgM and anti-PEG IgG

Anti-PEG IgM and IgG in rat serum were detected by ELISA. Briefly, each well of a Maxisorp 96-well microplate was coated with 5 μg/well PEG10000 in 100 μL PBS overnight at 4 °C. The coated plate was subsequently washed three times with 350 μL of wash buffer (0.05% (w/v) CHAPS in DPBS). Then, 200 μL of blocking buffer (5% (w/v) skim milk powder in DPBS) was added

followed by incubation at room temperature for 1.5 h. Plates were subsequently washed three times with 350 μL of wash buffer. Three times serial dilutions of rat anti-PEG IgM (rAGP6) and rat anti-PEG IgG (r33G) were prepared in dilution buffer (2% (w/v) skim milk powder in DPBS), respectively. Add 100 μL of rat serum samples diluted 1: 150 with dilution buffer and serially diluted rat anti-PEG IgM (rAGP6) and rat anti-PEG IgG (r33G) standards (in duplicate) to a 96-well plate and then incubated for 1 hour at room temperature. Plates were subsequently washed five times with 350 μL of wash buffer to remove unbound antibodies. 0.08 μg/mL of peroxidase-conjugated affinipure rabbit anti-rat IgM μ-chain specific and peroxidase-conjugated affinipure donkey anti-rat IgG (H+L) in 50 μL of dilution buffer was added to the IgM or IgG detection plates, respectively, and then incubated for 1 hour at room temperature. The plates were subsequently washed five times with 350 μL of wash buffer. Then, 100 μL of TMB was added to plates and incubated for 30 minutes at room temperature. After stopping the HRP reaction with 100 μL of 2 N H_2SO_4, the absorbance was measured at 450 nm (signal) and 570 nm (background) using a microplate reader (Thermo Fisher Scientific, Waltham, MA, USA). The absorbance at 450 nm was subtracted from the absorbance at 570 nm to calculate the corrected absorbance. The concentrations of anti-PEG IgG and anti-PEG IgM in serum samples were calculated using four-parameter logistic (4PL) curves for anti-PEG IgM (rAGP6) and anti-PEG IgG (r33G) fitted by Origin 2021, respectively. Assay precision was determined by calculating the mean coefficient of variation (CV%) for all detectable standard curve points and all samples.

Biodistribution of PEGylated LNP in major organs

Wistar rats were randomly divided into a control group and three experimental groups (n=6). On Day 0, experimental group 1 (L-LNP group) was injected intramuscularly with 0.009 mg phospholipids/kg DiR-LU@LNP; experimental group 2 (M-LNP group) was injected intramuscularly with 0.342 mg phospholipids/kg DiR-LU@LNP; experimental group 3 (H-LNP group) was injected intramuscularly with 2.358 mg phospholipids/kg DiR-LU@LNP; the control group received only PBS as a placebo control. On Day 21, each group was injected intramuscularly with the exact same dose of DiR-LU@LNP as the initial injection. Six hours after the first and second injections, three rats per group were injected intraperitoneally with D-luciferin at a dose of 150 mg/kg. Rats were sacrificed 15 minutes after administration of D-luciferin and immediately dissected and their primary organs, including heart, liver, spleen, lung, kidneys, draining lymph node and muscle at the injection site were collected for fluorescence and bioluminescence imaging using the IVIS Spectrum imaging system (Caliper Life Sciences). Whole-organ fluorescence imaging was performed by IVIS Spectrum imaging system using excitation/emission wavelengths of 745/800 nm to capture DiR fluorescence signal. Image analysis was conducted using Living Image software (Caliper Life Sciences). Organs were weighed, and their weights were recorded to normalize the total organ total fluorescence signal by organ mass.

Blood clearance of PEGylated LNP

Wistar rats were randomly divided into a control group and three experimental groups (n=3). On Day 0, experimental group 1 (L-LNP group) was injected intramuscularly with 0.009 mg phospholipids/kg DiR-LNP; experimental group 2 (M-LNP group) was injected intramuscularly with 0.342 mg phospholipids/kg DiR-LNP; experimental group 3 (H-LNP group) was injected intramuscularly with 2.358 mg phospholipids/kg DiR-LNP; control group received only PBS as a placebo control. On Day 21, each group was injected intramuscularly with the exact same dose of DiR-LNP as the initial injection. Peripheral blood samples were collected from the retro-orbital venous plexus at 5 minutes, 30 minutes, 1 hour, 3 hours, 6 hours, 10 hours, 24 hours and 48 hours after first and second injections. Blood samples were centrifuged at 2000×g at 4 °C for 15 minutes, and the obtained serum samples were immediately stored in dark at -80 °C. The fluorescence associated with LNP in serum samples was detected by fluorescent spectroscopy on a Spectramax ID5 (Molecular Devices, San Jose, California, USA) at excitation/emission wavelengths of 748/780 nm.

Statistical analysis

Statistical analyses were performed with Prism 9.2.0 (GraphPad Software) and R 4.0.5 (R Software). The concentrations of anti-PEG IgM and IgG were analyzed after log10 transformation. Changing curves of average level of antibody over time for four groups were fitted by the R package called "ggalt". Profile analysis was then performed to examine whether the overall trends of the average levels of antibodies over time between every two groups were equal. According to factorial design (group × time) and repeated measures of antibody levels, linear mixed models were conducted to compare the change rates and average levels of antibodies across groups, with all time points included. Linear mixed models considered variables including group (indicating mean differences in the average levels of antibodies), time, time^2, number of injections, and interaction term of group and time (indicating mean differences in the change rates of antibodies levels) as fixed effect and subject as random effect. Further, to compare the average levels of antibodies between each two groups at each time point, Mann-Whitney U tests were performed. The raw P values derived from the Mann-Whitney U tests were adjusted for false discovery rate (FDR) to control the increased rate of type I errors due to multiple comparisons. In addition, to compare the change rates and average levels of differences of anti-PEG IgM and anti-PEG IgG between two injections of PEGylated LNP, we repeated analyses abovementioned (including curve fitting, profile analysis, linear mixed model, and Mann-Whitney U test). In this part, linear mixed models considered variables including group, time, time^2, and interaction term of group and time as fixed effect and subject as random effect. In the biodistribution study and blood clearance study, statistical analysis was performed using multiple unpaired t tests with correction for multiple comparisons. All data are shown as means ± SD. $P < 0.05$ was considered statistically significant. Non-significant comparisons are not shown, unless otherwise noted as n.s. (not significant).

References

1. J.A. Kulkarni, D. Witzigmann, S.B. Thomson, S. Chen, B.R. Leavitt, P.R. Cullis, R. van der Meel, The current landscape of nucleic acid therapeutics. Nat. Nanotechnol. **16**, 630-643 (2021).
2. J. Szebeni, G. Storm, J.Y. Ljubimova, M. Castells, E.J. Phillips, K. Turjeman, Y. Barenholz, D.J.A. Crommelin, M.A. Dobrovolskaia, Applying lessons learned from nanomedicines to understand rare hypersensitivity reactions to mRNA-based SARS-CoV-2 vaccines. Nat. Nanotechnol. **17**, 337-346 (2022).
3. B.B. Mendes, J. Conniot, A. Avital, D. Yao, X. Jiang, X. Zhou, N. Sharf-Pauker, Y. Xiao, O. Adir, H. Liang, J. Shi, A. Schroeder, J. Conde, Nanodelivery of nucleic acids. Nat Rev Methods Primers **2**, (2022).
4. A. Curreri, D. Sankholkar, S. Mitragotri, Z. Zhao, RNA therapeutics in the clinic. Bioeng. Transl. Med., (2022).
5. J. S. Suk, Q. G. Xu, N. Kim, J. Hanes, L. M. Ensign, PEGylation as a strategy for improving nanoparticle-based drug and gene delivery. Adv. Drug. Deliver. Rev. **99**, 28-51 (2016).
6. A. Khurana, P. Allawadhi, I. Khurana, S. Allwadhi, R. Weiskirchen, A.K. Banothu, D. Chhabra, K. Joshi, K.K. Bharani, Role of nanotechnology behind the success of mRNA vaccines for COVID-19. Nano Today **38**, (2021).
7. A. W. Richter, E. Akerblom, Antibodies against polyethylene-glycol produced in animals by immunization with monomethoxy polyethylene-glycol modified proteins. Int. Arch. Aller. Imm. **70**, 124-131 (1983).
8. B. M. Chen, T. L. Cheng, S. R. Roffler, Polyethylene glycol immunogenicity: Theoretical, clinical, and practical aspects of anti-polyethylene glycol antibodies. Acs Nano **15**, 14022-14048 (2021).
9. H. F. Haddad, J. A. Burke, E. A. Scott, G. A. Ameer, Clinical Relevance of pre-existing and treatment-induced anti-poly(ethylene glycol) antibodies. Regen. Eng. Transl. Med. **8**, 32-42 (2022).
10. T.T.H. Thi, E.H. Pilkington, D.H. Nguyen, J.S. Lee, K.D. Park, N.P. Truong, The importance of poly(ethylene glycol) alternatives for overcoming PEG immunogenicity in drug delivery and bioconjugation. Polymers-Basel **12**, (2020).
11. A. S. Abu Lila, H. Kiwada, T. Ishida, The accelerated blood clearance (ABC) phenomenon: clinical challenge and approaches to manage. J. Control. Release **172**, 38-47 (2013).
12. T. L. Cheng, P. Y. Wu, M. F. Wu, J. W. Chern, S. R. Roffler, Accelerated clearance of polyethylene glycol-modified proteins by anti-polyethylene glycol IgM. Bioconjug. Chem. **10**, 520-528 (1999).
13. T. Ishida, M. Ichihara, X. Wang, K. Yamamoto, J. Kimura, E. Majima, H. Kiwada, Injection of PEGylated liposomes in rats elicits PEG-specific IgM, which is responsible for rapid elimination of a second dose of PEGylated liposomes. J. Control. Release **112**, 15-25 (2006).
14. J.K. Armstrong, G. Hempel, S. Koling, L.S. Chan, T. Fisher, H.J. Meiselman, G. Garratty, Antibody against poly(ethylene glycol) adversely affects PEG-asparaginase therapy in acute lymphoblastic leukemia patients. Cancer **110**, 103-111 (2007).
15. M.S. Hershfield, N.J. Ganson, S.J. Kelly, E.L. Scarlett, D.A. Jaggers, J.S. Sundy, Induced and pre-existing anti-polyethylene glycol antibody in a trial of every 3-week dosing of pegloticase for refractory gout, including in organ transplant recipients. Arthritis Res. Ther. **16**, R63 (2014).
16. X.P. Zhang, V. Goel, H. Attarwala, M.T. Sweetser, V.A. Clausen, G.J. Robbie, Patisiran pharmacokinetics, pharmacodynamics, and exposure-response analyses in the phase 3 APOLLO trial in patients with hereditary transthyretin-mediated (hATTR) amyloidosis. J. Clin. Pharmacol. **60**, 37-49 (2020).
17. Y. Ju, W.S. Lee, E.H. Pilkington, H.G. Kelly, S. Li, K.J. Selva, K.M. Wragg, K. Subbarao, T.H.O. Nguyen, L.C. Rowntree, L.F. Allen, K. Bond, D.A. Williamson, N.P. Truong, M.

Plebanski, K. Kedzierska, S. Mahanty, A.W. Chung, F. Caruso, A.K. Wheatley, J.A. Juno, S.J. Kent, Anti-PEG antibodies boosted in humans by SARS-CoV-2 lipid nanoparticle mRNA vaccine. Acs Nano **16**, 11769–11780 (2022).

18. G. Guerrini, S. Gioria, A.V. Sauer, S. Lucchesi, F. Montagnani, G. Pastore, A. Ciabattini, D. Medaglini, L. Calzolai, Monitoring anti-PEG antibodies level upon repeated lipid nanoparticle-based COVID-19 vaccine administration. Int. J. Mol. Sci. **23**, (2022).
19. J.M. Carreno, G. Singh, J. Tcheou, K. Srivastava, C. Gleason, H. Muramatsu, P. Desai, J.A. Aberg, R.L. Miller, P. Study Group, N. Pardi, V. Simon, F. Krammer, mRNA-1273 but not BNT162b2 induces antibodies against polyethylene glycol (PEG) contained in mRNA-based vaccine formulations. Vaccine **40**, 6114-6124 (2022).
20. Food and Drug Administration. ONPATTRO (patisiran) lipid complex injection addendum to drug product quality review, 14 February, 2017; https://www.accessdata.fda.gov/drugsatfda_docs/nda/2018/210922Orig1s000ChemR.pdf.
21. Food and Drug Administration. Comirnaty Information-Summary basis for regulatory action, 8 November, 2021; https://www.fda.gov/media/151733/download
22. Food and Drug Administration. Spikevax Information-Summary basis for regulatory action, 30 January, 2022; https://www.fda.gov/media/155931/download
23. M. Danaei, M. Dehghankhold, S. Ataei, F.H. Davarani, R. Javanmard, A. Dokhani, S. Khorasani, M.R. Mozafari, Impact of particle size and polydispersity index on the clinical applications of lipidic nanocarrier systems. Pharmaceutics **10**, 57 (2018).
24. Y. Eygeris, M. Gupta, J. Kim, G. Sahay, Chemistry of lipid nanoparticles for RNA delivery. Acc. Chem. Res. **55**, 2-12 (2022).
25. K. Yang, C. Reker-Smit, M. C. A. Stuart, A. Salvati, Effects of protein source on liposome uptake by cells: Corona composition and impact of the excess free proteins. Adv. Healthc. Mater. **10**, e2100370 (2021).
26. V.A. Naumenko, S.S. Vodopyanov, K.Y. Vlasova, D.M. Potashnikova, P.A. Melnikov, D.A. Vishnevskiy, A.S. Garanina, M.P. Valikhov, A.V. Lipatova, V.P. Chekhonin, A.G. Majouga, M.A. Abakumov, Intravital imaging of liposome behavior upon repeated administration: A step towards the development of liposomal companion diagnostic for cancer nanotherapy. J. Control. Release **330**, 244-256 (2021).
27. M. Ibrahim, E. Ramadan, N.E. Elsadek, S.E. Emam, T. Shimizu, H. Ando, Y. Ishima, O.H. Elgarhy, H.A. Sarhan, A.K. Hussein, T. Ishida, Polyethylene glycol (PEG): The nature, immunogenicity, and role in the hypersensitivity of PEGylated products. J. Control. Release **351**, 215-230 (2022).
28. Q. Yang, S.K. Lai, Anti-PEG immunity: emergence, characteristics, and unaddressed questions. Wiley Interdiscip. Rev. Nanomed. Nanobiotechnol. **7**, 655-677 (2015).
29. B.M. Chen, Y.C. Su, C.J. Chang, P.A. Burnouf, K.H. Chuang, C.H. Chen, T.L. Cheng, Y.T. Chen, J.Y. Wu, S.R. Roffler, Measurement of pre-existing IgG and IgM antibodies against polyethylene glycol in healthy individuals. Anal. Chem. **88**, 10661-10666 (2016).
30. Q. Yang, T.M. Jacobs, J.D. McCallen, D.T. Moore, J.T. Huckaby, J.N. Edelstein, S.K. Lai, Analysis of Pre-existing IgG and IgM antibodies against polyethylene glycol (PEG) in the general population. Anal. Chem. **88**, 11804-11812 (2016).
31. D. Shi, D. Beasock, A. Fessler, J. Szebeni, J.Y. Ljubimova, K.A. Afonin, M.A. Dobrovolskaia, To PEGylate or not to PEGylate: Immunological properties of nanomedicine's most popular component, polyethylene glycol and its alternatives. Adv. Drug Deliver. Rev. **180**, 114079 (2022)
32. World Health Organization. WHO guidelines on non-clinical evaluation of vaccines, WHO Technical Report Series No. 927, Annex 1, 1 January 2005; https://cdn.who.int/media/docs/default-source/biologicals/vaccine-standardization/annex-1nonclinical.p31-63.pdf?sfvrsn=e87c28d8_3&download=true

33. European Medicines Agency. Spikevax (previously COVID-19 Vaccine Moderna) : EPAR - Public assessment report, 20 January 2021; https://www.ema.europa.eu/en/documents/assessment-report/spikevax-previously-covid-19-vaccine-moderna-epar-public-assessment-report_en.pdf
34. European Medicines Agency. Comirnaty : EPAR - Public assessment report, 23 December 2020; https://www.ema.europa.eu/en/documents/assessment-report/comirnaty-epar-public-assessment-report_en.pdf
35. G.T. Kozma, T. Shimizu, T. Ishida, J. Szebeni, Anti-PEG antibodies: Properties, formation, testing and role in adverse immune reactions to PEGylated nano-biopharmaceuticals. Adv. Drug Deliver. Rev.**154**, 163-175 (2020).
36. T. Defrance, M. Taillardet, L. Genestier, T cell-independent B cell memory. Curr. Opin. Immunol. **23**, 330-336 (2011).
37. M. Ichihara, T. Shimizu, A. Imoto, Y. Hashiguchi, Y. Uehara, T. Ishida, H. Kiwada, Anti-PEG IgM response against PEGylated liposomes in mice and rats. Pharmaceutics **3**, 1-11 (2010).
38. K.R. Alugupalli, J.M. Leong, R.T. Woodland, M. Muramatsu, T. Honjo, R.M. Gerstein, B1b lymphocytes confer T cell-independent long-lasting immunity. Immunity **21**, 379-390 (2004).
39. T.V. Obukhanych, M.C. Nussenzweig, T-independent type II immune responses generate memory B cells. J. Exp. Med. **203**, 305-310 (2006).
40. M. Taillardet, G. Haffar, P. Mondiere, M.J. Asensio, H. Gheit, N. Burdin, T. Defrance, L. Genestier, The thymus-independent immunity conferred by a pneumococcal polysaccharide is mediated by long-lived plasma cells. Blood **114**, 4432-4440 (2009).
41. N.N. Zhang, X.F. Li, Y.Q. Deng, H. Zhao, Y.J. Huang, G. Yang, W.J. Huang, P. Gao, C. Zhou, R.R. Zhang, Y. Guo, S.H. Sun, H. Fan, S.L. Zu, Q. Chen, Q. He, T.S. Cao, X.Y. Huang, H.Y. Qiu, J.H. Nie, Y.H. Jiang, H.Y. Yan, Q. Ye, X. Zhong, X.L. Xue, Z.Y. Zha, D.S. Zhou, X. Yang, Y.C. Wang, B. Ying, C.F. Qin, A thermostable mRNA vaccine against COVID-19. Cell **182**, 1271-1283 (2020).
42. J. C. M. Stewart, Colorimetric Determination of phospholipids with ammonium ferrothiocyanate. Anal. Biochem. **104**, 10-14 (1980).
43. A. Nair, M.A. Morsy, S. Jacob, Dose translation between laboratory animals and human in preclinical and clinical phases of drug development. Drug. Dev. Res. **79**, 373-382 (2018)

Figures and Tables

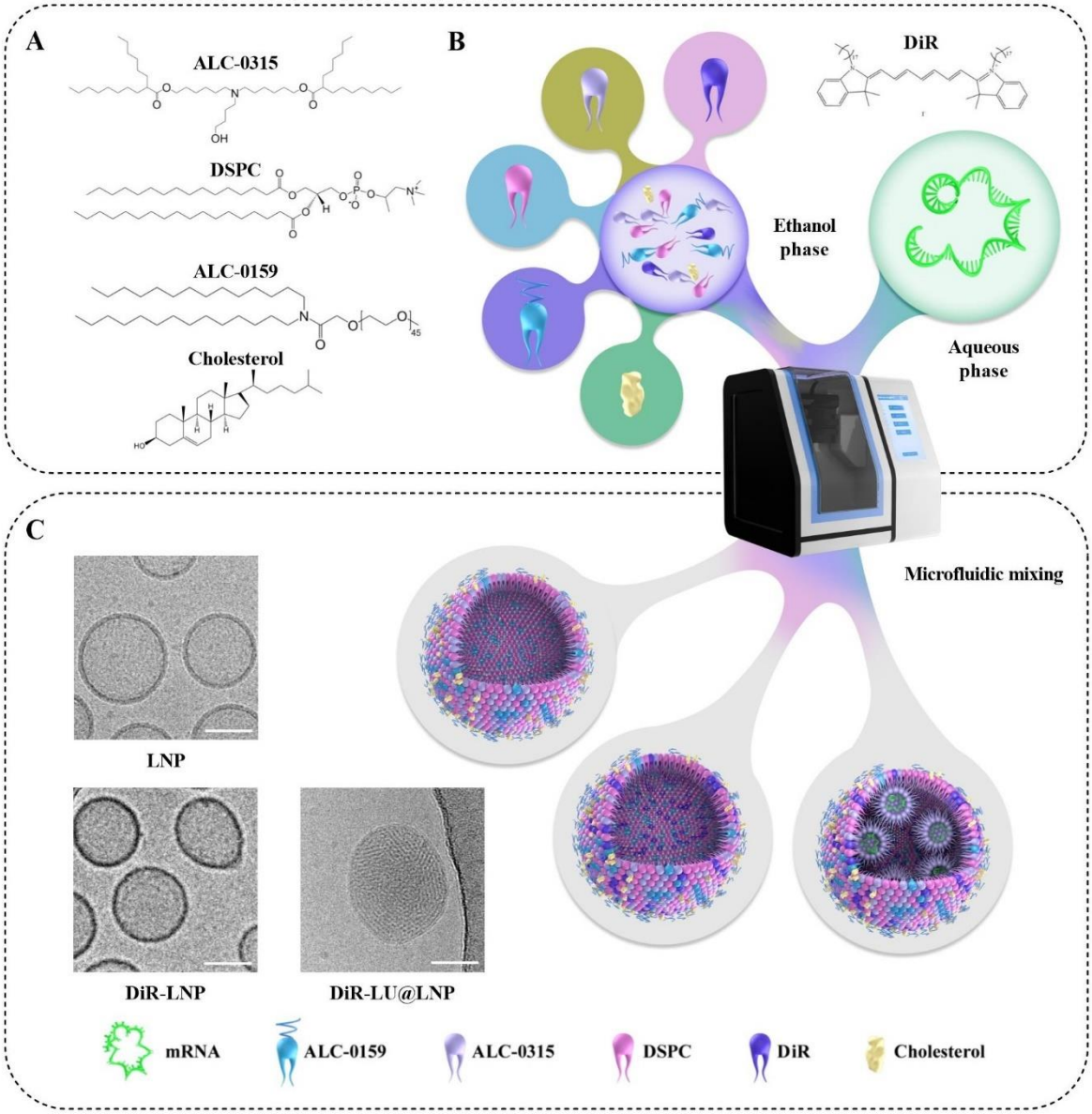

Fig. 1. Preparation of LNP, DiR-LNP and DiR-LU@LNP. (**A**) Chemical structures of lipids in BNT162b2 COVID-19 vaccine. (**B**) Schematic illustration of the synthesis of LNP, DiR-LNP and DiR-LU@LNP. Briefly, the ethanol phase was combined with the aqueous phase at a flow rate ratio of 1: 3 (ethanol: aqueous) through a microfluidic mixing device. (**C**) Representative cryogenic transmission electron microscopy (cryo-TEM) images of LNP, DiR-LNP and DiR-LU@LNP. Scale bar: 50 nm

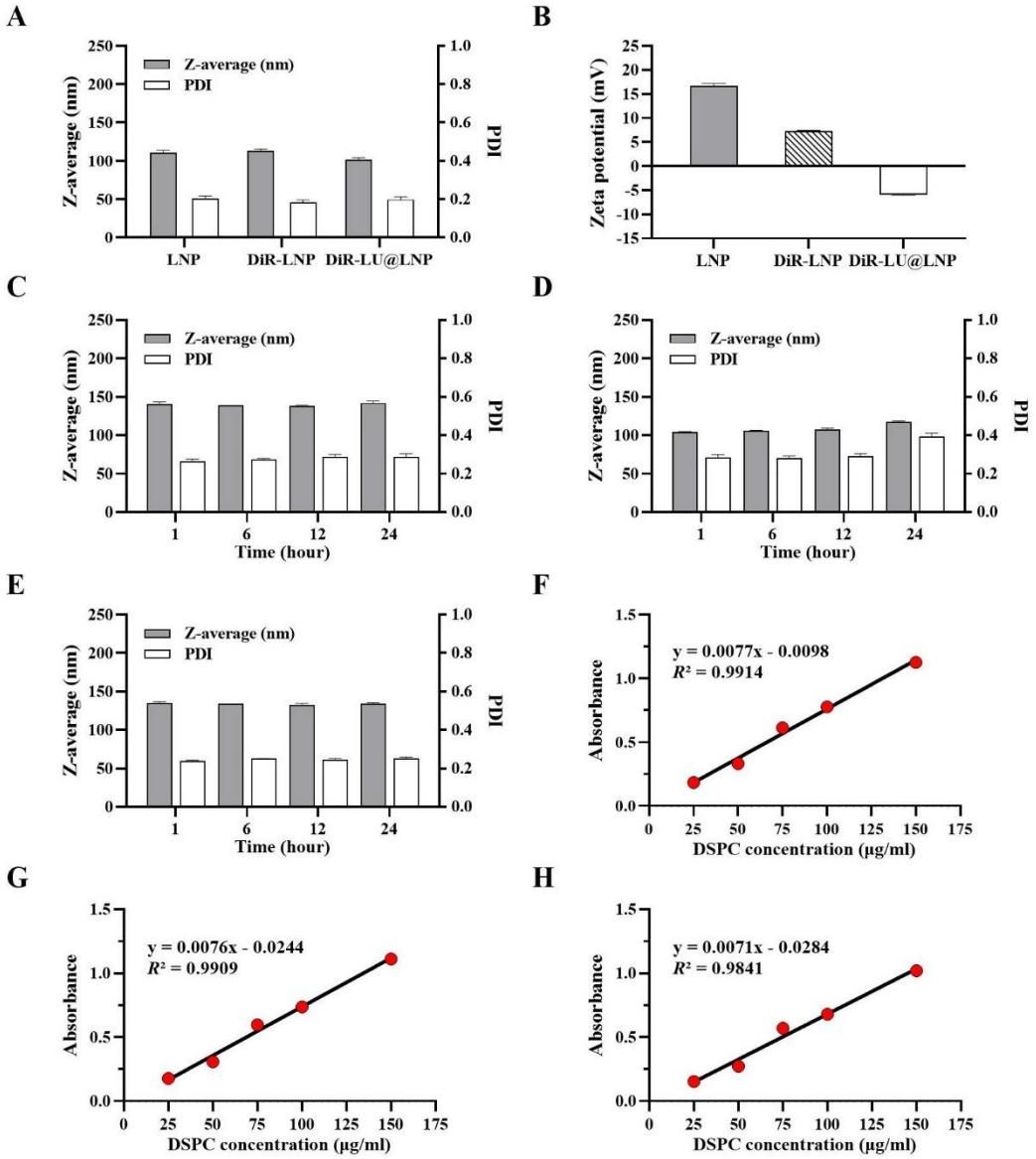

Fig. 2. Characterization of LNP, DiR-LNP and DiR-LU@LNP. (**A**) Hydrodynamic size (Z-average) and polydispersity index (PDI) of LNP, DiR-LNP and DiR-LU@LNP measured by DLS. (**B**) Zeta potential of LNP, DiR-LNP and DiR-LU@LNP. (C-E) Detection of the stability of (C) LNP, (D) DiR-LNP and (E) DiR-LU@LNP in serum. LNP, DiR-LNP and DiR-LU@LNP were incubated in PBS containing 10% rat serum at 37°C for the indicated time points and 1 mL of nanoparticle solution was taken to characterize the Z-average and PDI of LNP, DiR-LNP and DiR-LU@LNP by DLS, respectively. (**F-H**) Standard curves for measuring phospholipid (DSPC) concentrations in (F) LNP, (G) DiR-LNP and (H) DiR-LU@LNP solutions. Data are represented as the mean and standard deviation of three technical repeats.

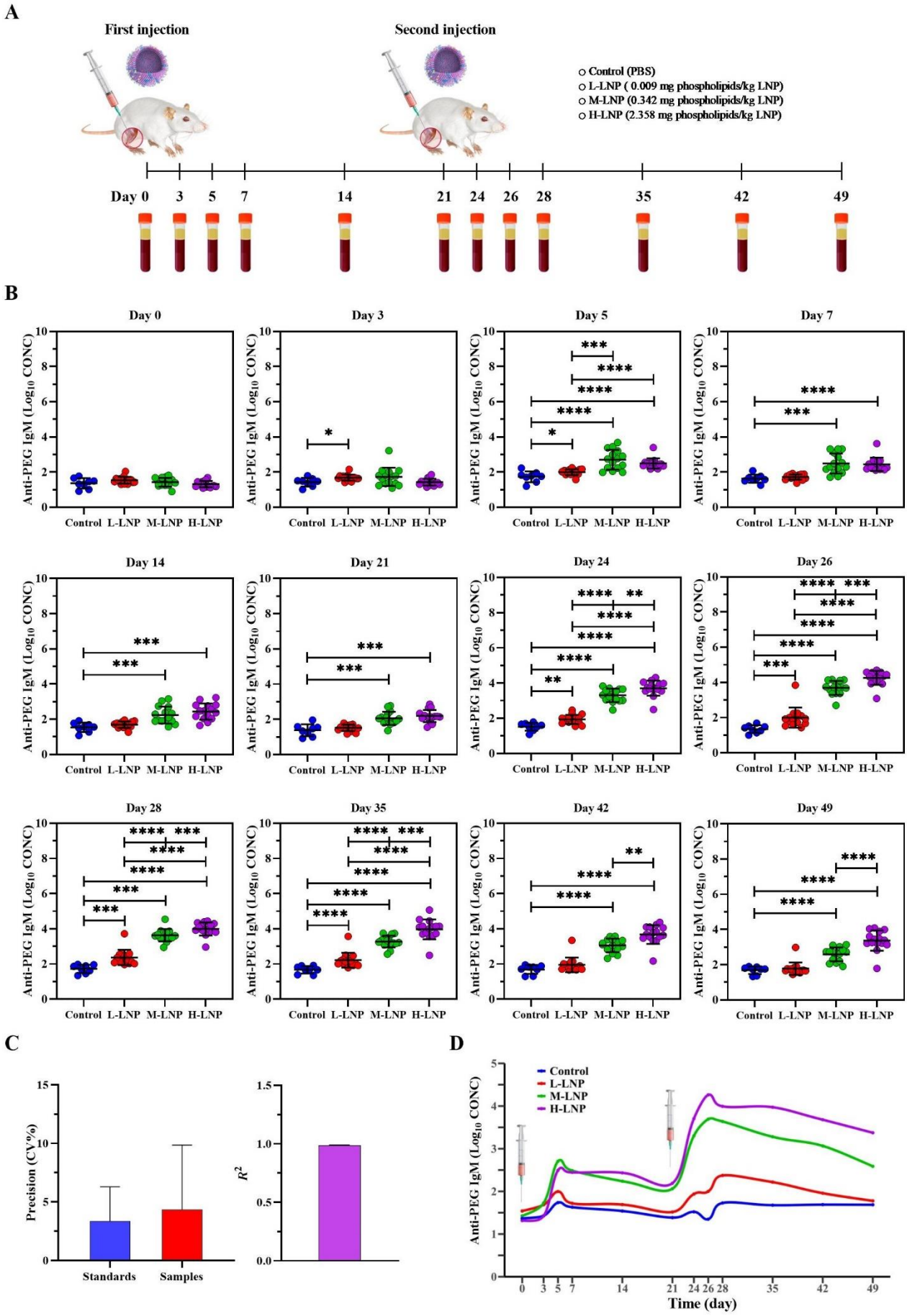
A
First injection
Second injection
Control (PBS)
L-LNP (0.009 mg phospholipids/kg LNP)
M-LNP (0.342 mg phospholipids/kg LNP)
H-LNP (2.358 mg phospholipids/kg LNP)
Day 0
3
5
7
14
21
24
26
28
35
42
49
B
Day 0
Day 3
Day 5
Day 7
Day 14
Day 21
Day 24
Day 26
Day 28
Day 35
Day 42
Day 49
Anti-PEG IgM (Log10 CONC)
Control
L-LNP
M-LNP
H-LNP
C
Precision (CV%)
Standards
Samples
R2
D
Control
L-LNP
M-LNP
H-LNP
Anti-PEG IgM (Log10 CONC)
Time (day)

Fig. 3. Administration protocols of PEGylated LNP and induction of anti-PEG antibody in rat. (**A**) Schematic illustration of the experimental design. Wistar rats were injected intramuscularly with 0.009, 0.342 or 2.358 mg phospholipids/kg LNP twice on Day 0 and Day 21. Rats in the control group were injected with PBS. Serum was collected at the indicated time points (Day 0, 3, 5, 7, 14, 21, 24, 26, 28, 35, 42 and 49). Anti-PEG IgM and Anti-PEG IgG were detected by ELISA in rat serum at each time points. (**B**) Quantitative analysis of anti-PEG IgM in rat serum at each time point. Anti-PEG IgM (Log_{10} CONC) means the log10-transformed concentration of anti-PEG IgM. (**C**) Details of ELISA assay for anti-PEG IgM. The image on the left shows the average precision (CV%) of standards and samples in the ELISA assay. The image on the right shows the mean linear regression coefficient of determination (R^2) of the standard curve for ELISA. (**D**) Time-course of anti-PEG IgM production induced by the repeated injection of PEGylated LNP. The changing curves of mean anti-PEG IgM (Log_{10} CONC) levels over time were fitted by the R package called "ggalt". The mean and standard deviation of n = 15 are shown with the exception of the control group, where n = 8. Differences in Anti-PEG IgM (Log_{10} CONC) between each two groups at each time point were compared using the Mann-Whitney U test, with *P* values adjusted for FDR (**P* < 0.05, ***P* < 0.01, ****P* < 0.001, **** *P* < 0.0001). CONC: concentration; FDR: false discovery rate; CV: coefficient of variation.

Table 1. Linear mixed model analysis of change in the anti-PEG IgM level after injection of PEGylated LNP over time across groups.

Variable	Anti-PEG IgM					
	β (95% CI)	*P*	β (95% CI)	*P*	β (95% CI)	*P*
Group						
Control	0 (ref.)	-	-	-	-	-
L-LNP	0.2337 (-0.0351, 0.5025)	0.0915	0 (ref.)	-	-	-
M-LNP	0.6198 (0.3509, 0.8886)	<0.0001	0.3861 (0.1618, 0.6103)	0.0011	0 (ref.)	-
H-LNP	0.4103 (0.1415, 0.6792)	0.0035	0.1767 (-0.0476, 0.4009)	0.1257	-0.2094 (-0.4336, 0.0148)	0.0701
Time	0.0140 (0.0032, 0.0249)	0.0116	-	-	-	-
Time^2	-0.0008 (-0.0009, -0.0006)	<0.0001	-	-	-	-
Group*Time						
Control*Time	0 (ref.)	-	-	-	-	-
L-LNP*Time	0.0034 (-0.0036, 0.0105)	0.3408	0 (ref.)	-	-	-
M-LNP*Time	0.0238 (0.0167, 0.0308)	<0.0001	0.0203 (0.0145, 0.0262)	<0.0001	0 (ref.)	-
H-LNP*Time	0.0458 (0.0387, 0.0528)	<0.0001	0.0424 (0.0365, 0.0482)	<0.0001	0.0220 (0.0161, 0.0279)	<0.0001
Injection						
First	0 (ref.)	-	-	-	-	-
Second	0.9166 (0.7852, 1.0479)	<0.0001	-	-	-	-

Models considered variables including group, time, time^2, number of injections, and interaction term of group and time as fixed effect and subject as random effect. β for group represents mean differences in antibody levels between groups at all time points. β for time and time^2 represents rate of change in antibody levels over time for the four groups at all time points. β for injection represents mean difference in antibody levels for the four groups at all time points between the first injection and second injection. β for group*time represents mean differences in the rate of change of antibody levels over time between groups. ref: reference.

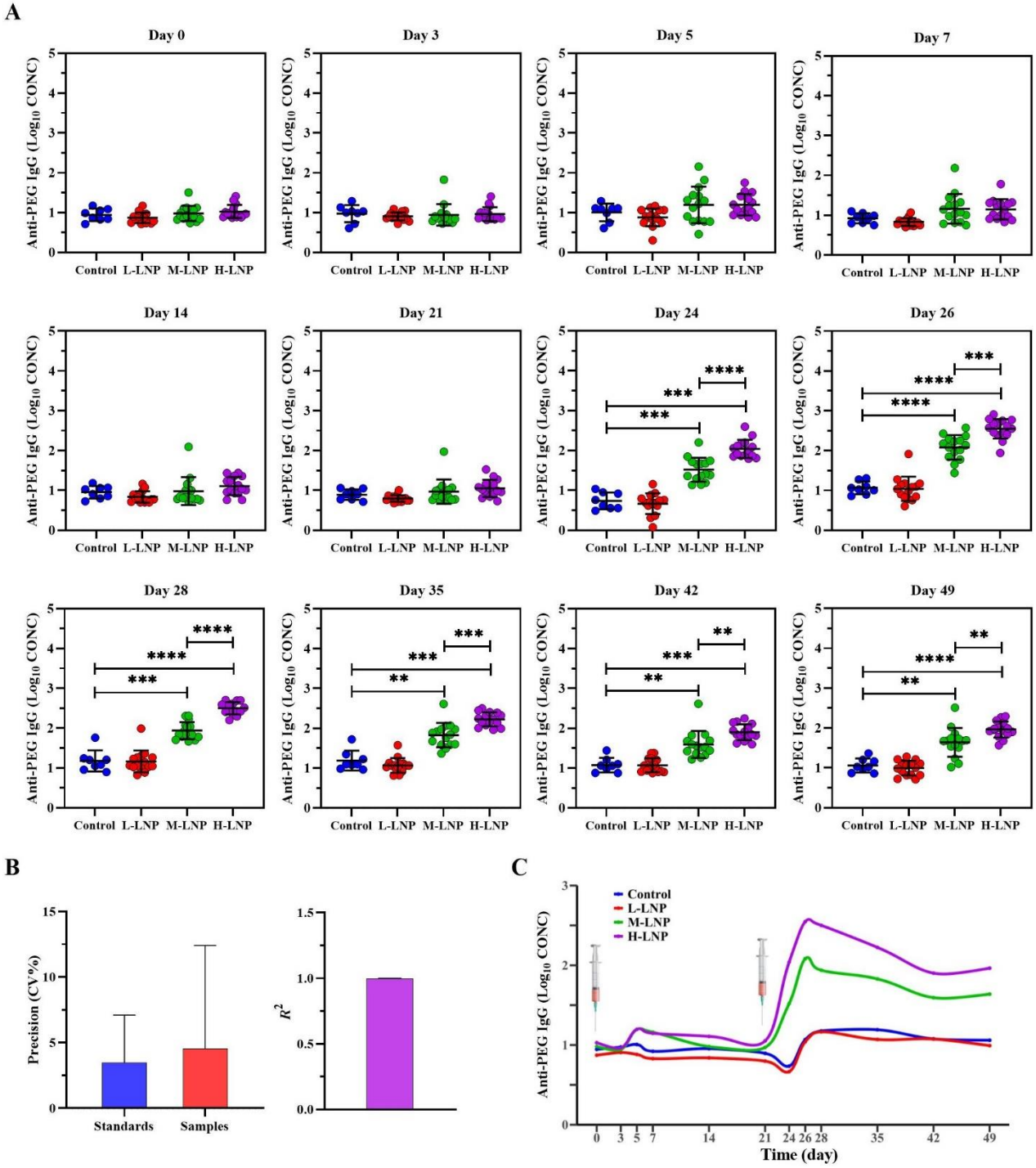

Fig. 4. Induction of anti-PEG IgG by PEGylated LNP in rat. (**A**) Quantitative analysis of anti-PEG IgG in rat serum at each time point. Anti-PEG IgG (Log_{10} CONC) means the log10-transformed concentration of anti-PEG IgG. (**B**) Details of ELISA assay for anti-PEG IgG. The image on the left shows the average precision (CV%) of standards and samples in the ELISA assay. The image on the right shows the mean linear regression coefficient of determination (R^2) of the standard curve for ELISA. (**C**) Time-course of anti-PEG IgG production induced by the repeated injection of PEGylated LNP. The changing curves of mean anti-PEG IgG (Log_{10} CONC) levels over time were fitted by the R package called "ggalt". The mean and standard deviation of n = 15 are shown with the exception of the control group, where n = 8. Differences in Anti-PEG IgG (Log_{10} CONC) between each two groups at each time point were compared using the Mann-Whitney U test, with P values adjusted for FDR (*$P < 0.05$, **$P < 0.01$, ***$P < 0.001$, **** $P < 0.0001$). CONC: concentration; FDR: false discovery rate.

Table 2. Linear mixed model analysis of change in the anti-PEG IgG level after injection of PEGylated LNP over time across groups.

Variable	Anti-PEG IgG					
	β (95% CI)	*P*	β (95% CI)	*P*	β (95% CI)	*P*
Group						
Control	0 (ref.)	-	-	-	-	-
L-LNP	-0.0950 (-0.2748, 0.0848)	0.3033	0 (ref.)	-	-	-
M-LNP	0.0871 (-0.0927, 0.2669)	0.3449	0.1821 (0.0321, 0.332)	0.0195	0 (ref.)	-
H-LNP	0.1230 (-0.0568, 0.3028)	0.1835	0.2179 (0.068, 0.3679)	0.0054	0.0359 (-0.1141, 0.1858)	0.6404
Time	-0.0092 (-0.0159, -0.0024)	0.0077	-	-	-	-
Time^2	-0.0001 (-0.0002, -0.00002)	0.0197	-	-	-	-
Group*Time						
Control*Time	0 (ref.)	-	-	-	-	-
L-LNP*Time	0.0011 (-0.0033, 0.0054)	0.6339	0 (ref.)	-	-	-
M-LNP*Time	0.0149 (0.0105, 0.0193)	< 0.0001	0.0138 (0.0102, 0.0175)	< 0.0001	0 (ref.)	-
H-LNP*Time	0.0244 (0.0200, 0.0288)	< 0.0001	0.0233 (0.0197, 0.027)	< 0.0001	0.0095 (0.0059, 0.0131)	< 0.0001
Injection						
First	0 (ref.)	-	-	-	-	-
Second	0.6549 (0.5734, 0.7364)	< 0.0001	-	-	-	-

Models considered variables including group, time, time^2, number of injections, and interaction term of group and time as fixed effect and subject as random effect. β for group represents mean differences in antibody levels between groups at all time points. β for time and time^2 represents rate of change in antibody levels over time for the four groups at all time points. β for injection represents mean difference in antibody levels for the four groups at all time points between the first injection and second injection. β for group*time represents mean differences in the rate of change of antibody levels over time between groups. ref: reference.

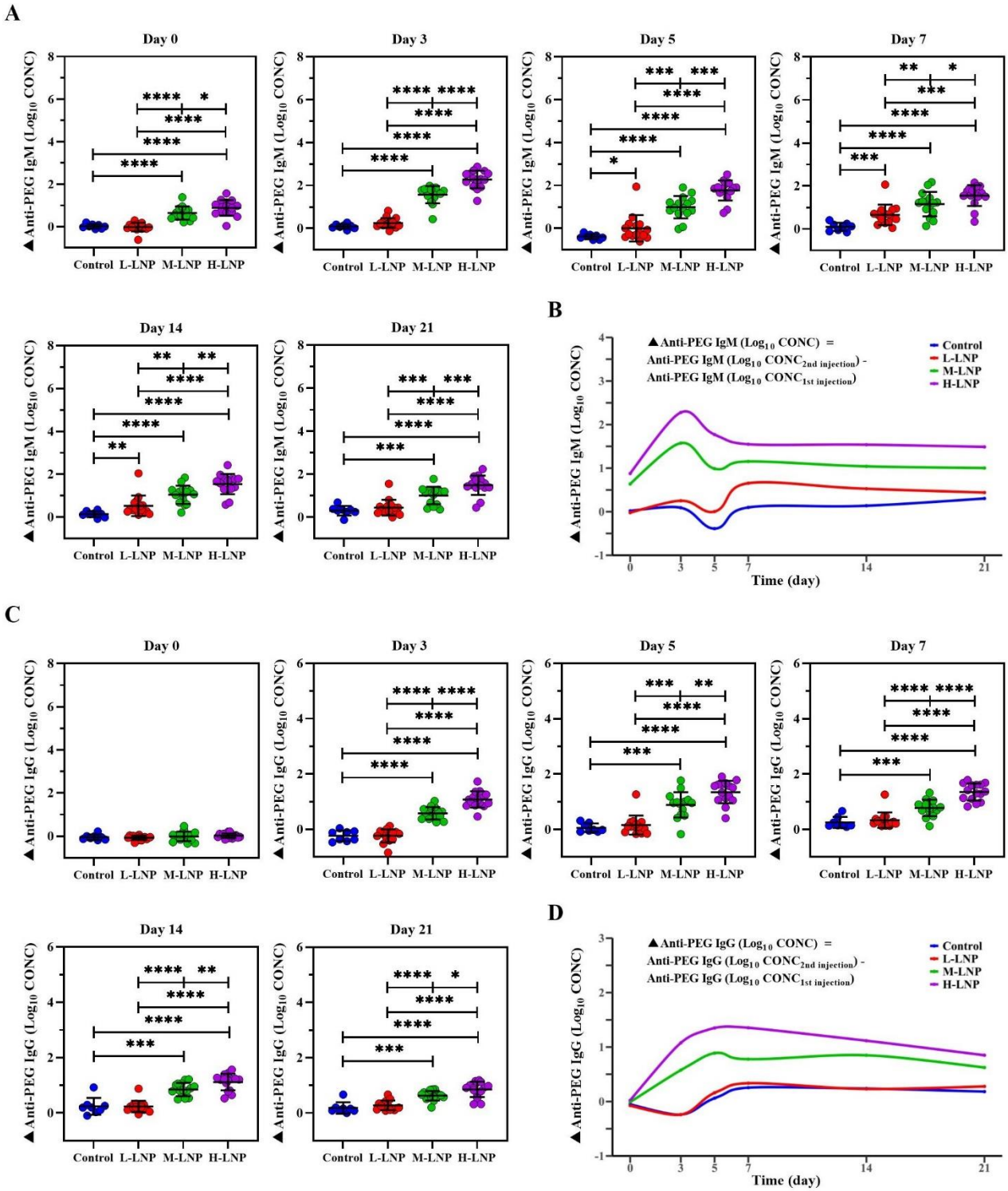

Fig. 5. Enhancement of anti-PEG IgM and anti-PEG IgG production by immunological memory induced by PEGylated LNP. (**A**) Enhanced anti-PEG IgM response induced by immunological memory. ▲Anti-PEG IgM (Log_{10} CONC) means the log10-transformed concentration of anti-PEG IgM (Anti-PEG IgM (Log_{10} $CONC_{2nd\ injection}$)) at designated time points after the second injection of PEGylated LNP respectively subtracted log_{10}-transformed concentrations of anti-PEG IgM (Anti-PEG IgM (Log_{10} $CONC_{1st\ injection}$)) at corresponding time points after the first injection of PEGylated LNP. (**B**) Time-course of an enhanced anti-PEG IgM response induced by immunological memory after the first injection of PEGylated LNP. (**C**) Enhanced anti-PEG IgG response induced by immunological memory. ▲Anti-PEG IgG (Log_{10} CONC) means log10-transformed concentrations of anti-PEG IgG (Anti-PEG IgG (Log_{10} $CONC_{2nd}$

$_{injection}$)) at designated time points after the second injection of PEGylated LNP respectively subtracted log_{10}-transformed concentrations of anti-PEG IgG (Anti-PEG IgG (Log_{10} $CONC_{1st\ injection}$)) at corresponding time points after the first injection of PEGylated LNP. (**D**) Time-course of the enhanced anti-PEG IgG response induced by immunological memory after the first injection of PEGylated LNP. The changing curves of ▲Anti-PEG IgM (Log_{10} CONC) and ▲Anti-PEG IgG (Log_{10} CONC) over time were fitted by the R package called "ggalt". The mean and standard deviation of n = 15 are shown with the exception of the control group, where n = 8. Differences in ▲Anti-PEG IgM (Log_{10} CONC) and ▲Anti-PEG IgG (Log_{10} CONC) between each two groups at each time point were compared using the Mann-Whitney U test, with *P* values adjusted for FDR (**P* < 0.05, ***P* < 0.01, ****P* < 0.001, **** *P* < 0.0001). CONC: concentration; FDR: false discovery rate.

Table 3. Linear mixed model analysis of change in the difference of anti-PEG IgM level (▲Anti-PEG IgM) between two injections of PEGylated LNP over time across groups.

Variable	▲Anti-PEG IgM					
	β (95% CI)	*P*	β (95% CI)	*P*	β (95% CI)	*P*
Group						
Control	0 (ref.)	-	-	-	-	-
L-LNP	0.2281 (-0.0915, 0.5477)	0.1653	0 (ref.)	-	-	-
M-LNP	1.1623 (0.8427, 1.4819)	< 0.0001	0.9343 (0.6677, 1.2008)	< 0.0001	0 (ref.)	-
H-LNP	1.6775 (1.3579, 1.9971)	< 0.0001	1.4494 (1.1828, 1.716)	< 0.0001	0.5152 (0.2486, 0.7817)	0.0003
Time	0.0725 (0.0441, 0.1009)	< 0.0001	-	-	-	-
Time^2	-0.0026 (-0.0037, -0.0015)	< 0.0001	-	-	-	-
Group*Time						
Control*Time	0 (ref.)	-	-	-	-	-
L-LNP*Time	0.0045 (-0.0156, 0.0247)	0.6596	0 (ref.)	-	-	-
M-LNP*Time	-0.0167 (-0.0369, 0.0034)	0.1048	-0.0213 (-0.0381, -0.0045)	0.0138	0 (ref.)	-
H-LNP*Time	-0.0165 (-0.0367, 0.0037)	0.1099	-0.021 (-0.0379, -0.0042)	0.0149	0.0002 (-0.0166, 0.0171)	0.9775

Models considered variables including group, time, time^2, and interaction term of group and time as fixed effect and subject as random effect. β for group represents mean differences in the difference of antibody levels between two injections among groups at all time points. β for time and time^2 represents rate of change in the difference of antibody levels between two injections over time for the four groups at all time points. β for group*time represents mean differences in the rate of change of the difference of antibody levels between two injections over time between groups. ref: reference.

Table 4. Linear mixed model analysis of change in the difference of anti-PEG IgG level (▲Anti-PEG IgG) between two injections of PEGylated LNP over time across groups.

Variable	▲Anti-PEG IgG					
	β (95% CI)	*P*	β (95% CI)	*P*	β (95% CI)	*P*
Group						
Control	0 (ref.)	-	-	-	-	-
L-LNP	0.0149 (-0.1866, 0.2164)	0.8847	0 (ref.)	-	-	-
M-LNP	0.5180 (0.3165, 0.7195)	< 0.0001	0.503 (0.335, 0.6711)	< 0.0001	0 (ref.)	-
H-LNP	0.8861 (0.6846, 1.0876)	< 0.0001	0.8711 (0.7031, 1.0392)	< 0.0001	0.3681 (0.2, 0.5362)	< 0.0001
Time	0.1232 (0.1022, 0.1442)	< 0.0001	-	-	-	-
Time^2	-0.0050 (-0.0058, -0.0042)	< 0.0001	-	-	-	-
Group*Time						
Control*Time	0 (ref.)	-	-	-	-	-
L-LNP*Time	0.0031 (-0.0118, 0.0180)	0.6848	0 (ref.)	-	-	-
M-LNP*Time	0.0030 (-0.0119, 0.0179)	0.6899	-0.0001 (-0.0125, 0.0124)	0.9933	0 (ref.)	-
H-LNP*Time	0.0002 (-0.0147, 0.0151)	0.9832	-0.0029 (-0.0154, 0.0095)	0.6445	-0.0029 (-0.0153, 0.0096)	0.6505

Models considered variables including group, time, time^2, and interaction term of group and time as fixed effect and subject as random effect. β for group represents mean differences in the difference of antibody levels between two injections among groups at all time points. β for time and time^2 represents rate of change in the difference of antibody levels between two injections over time for the four groups at all time points. β for group*time represents mean differences in the rate of change of the difference of antibody levels between two injections over time between groups. ref: reference.

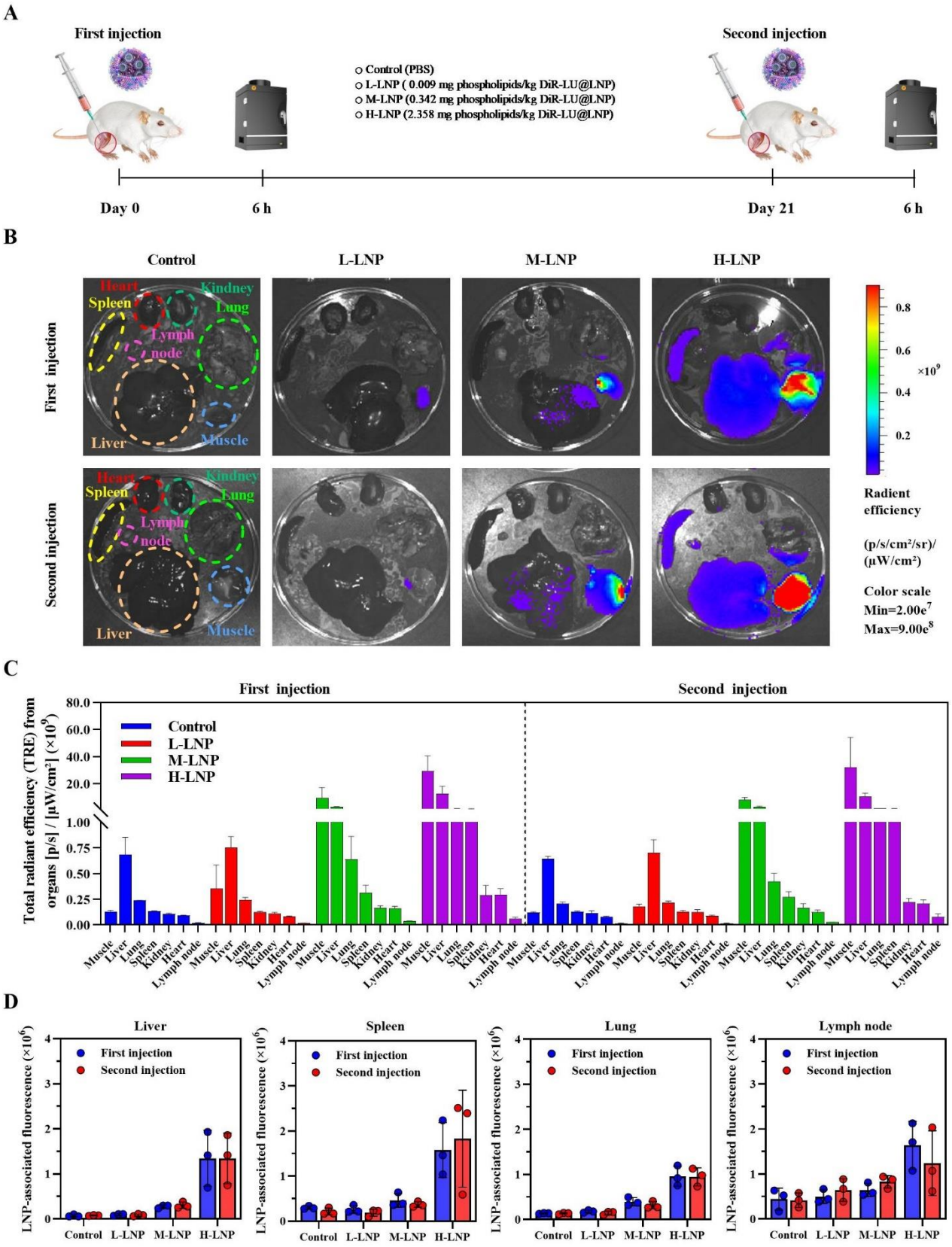

Fig. 6. Biodistribution of PEGylated LNP in major organs of rat. (**A**) Schematic illustration of the experimental design. Wistar rats were injected intramuscularly twice on Day 0 and Day 21 with 0.009, 0.342 or 2.358 mg phospholipids/kg DiR-LU@LNP. Rats in the control group were injected with PBS. 6 hours after the first and second injections, three rats from each group were sacrificed and immediately dissected. The major organs, including heart, liver, spleen, lung, kidneys, draining

lymph node and muscle at the injection site were collected for fluorescence imaging with IVIS Spectrum imaging system. (**B**) Representative whole-organ fluorescence images of rats 6 hours after each intramuscular injection of DiR-LU@LNP. (**C**) Total radiant efficiency (TRE) of organs 6 hours after the first injection and 6 hours after the second injection of DiR-LU@LNP. (**D**) Quantification of DiR-LU@LNP accumulation in the reticuloendothelial system (RES) 6 hours after the first and second intramuscular injections of DiR-LU@LNP. LNP-associated fluorescence was normalized by dividing the total radiant efficiency (TRE) by the mass from organs. All data represent the mean ± standard deviation (n = 3). Statistical analysis was performed using multiple unpaired *t* tests with correction for multiple testing (*$P < 0.05$, **$P < 0.01$, ***$P < 0.001$, **** $P < 0.0001$).

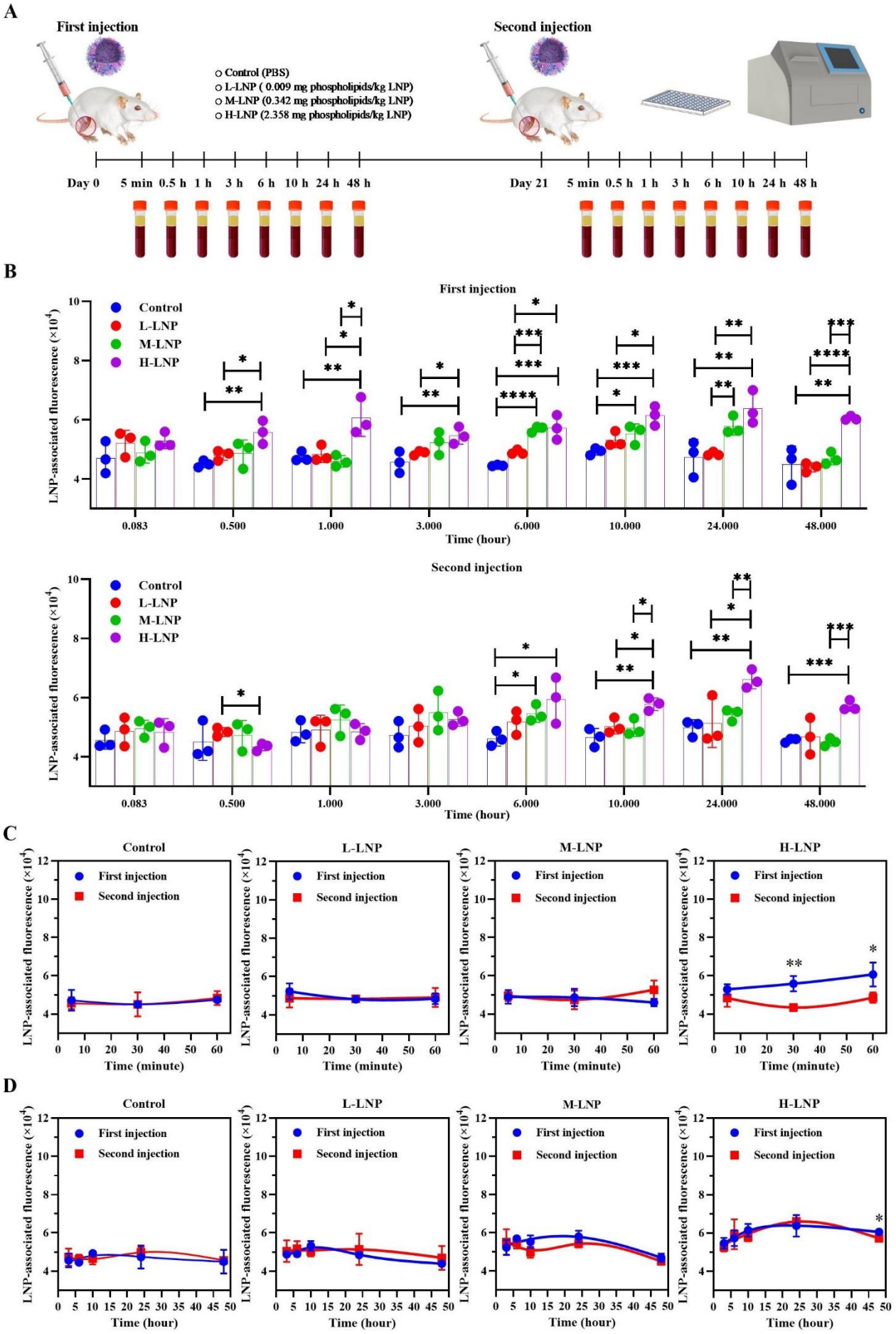
A
First injection
Second injection
Control (PBS)
L-LNP (0.009 mg phospholipids/kg LNP)
M-LNP (0.342 mg phospholipids/kg LNP)
H-LNP (2.358 mg phospholipids/kg LNP)
Day 0
5 min
0.5 h
1 h
3 h
6 h
10 h
24 h
48 h
Day 21
B
First injection
Second injection
Control
L-LNP
M-LNP
H-LNP
LNP-associated fluorescence (×10^4)
Time (hour)
0.083
0.500
1.000
3.000
6.000
10.000
24.000
48.000
C
Control
L-LNP
M-LNP
H-LNP
First injection
Second injection
LNP-associated fluorescence (×10^4)
Time (minute)
D
Time (hour)

Fig. 7. Blood clearance of PEGylated LNP in rats. (**A**) Schematic illustration of the experimental design. Wistar rats were injected intramuscularly twice with 0.009, 0.342 or 2.358 mg phospholipids/kg DiR-LNP on Day 0 and Day 21. Rats in the control group were injected with PBS. Serum was collected at 5 minutes, 30 minutes, 1 hour, 3 hours, 6 hours, 10 hours, 24 hours and 48 hours after the first and second injections and LNP-associated fluorescence in serum samples was detected by Spectramax ID5 fluorescent spectrometry. (**B**) LNP-associated fluorescence in serum samples collected at the above time points was detected by fluorescent spectroscopy with Spectramax ID5. (**C, D**) Blood clearance profile of DiR-LNP in rats. Fitted curves were created by Prism 9.2.0 (GraphPad Software). All data represent the mean ± standard deviation (n = 3). Differences in LNP-associated fluorescence between each two groups at each time point and differences in LNP-associated fluorescence between first injection and second injection at each time point were compared using the multiple unpaired *t* test, with *P* values adjusted for FDR (**P* < 0.05, ***P* < 0.01, ****P* < 0.001, **** *P* < 0.0001).